Supplementary Materials for

Miniaturized neural system for chronic, local intracerebral drug delivery

Canan Dagdeviren, Khalil B. Ramadi, Pauline Joe, Kevin Spencer, Helen N. Schwerdt, Hideki Shimazu, Sebastien Delcasso, Ken-ichi Amemori, Carlos Nunez-Lopez, Ann M. Graybiel, Michael J. Cima,* Robert Langer*

*Corresponding author. Email: mjcima@mit.edu (M.J.C.); rlanger@mit.edu (R.L.)

This PDF file includes:

Fig. S21. High-performance liquid chromatography absorbance spectrum at various concentrations of muscimol.
Fig. S22. Behavioral study on rat models.
Fig. S23. Average waveforms during distinctive infusions in a NHP.
Fig. S24. Distinctive infusion effect on firing rate in a NHP.
Fig. S25. LFP power analysis of a NHP trial.
Fig. S26. Plot of dose/volume delivered in previous studies reported in the literature, injecting muscimol into the SN compared to MiNDS.
Table S1. Statistical analysis for muscimol inhibition of spike activity for two sessions in two rats and for two sessions in a NHP.
References (*49–53*)

Materials and Methods

Resistivity Measurements

An impedance measurement system (Keysight E4980A) was used to measure the resistance and reactance of the S- and L-MiNDSs at 5 mV with a frequency sweep of 201 data points from 100 Hz to 100 kHz. The measurements were performed by submerging the tip of the MiNDS into a saline bath (0.9% sodium chloride, Baxter) and connecting the tungsten electrode to one of the analyzer terminals. The second analyzer terminal was submerged in the same saline bath, ensuring no physical contact with the MiNDS (fig. S7A). The impedance testing for each of the MiNDSs was repeated four times to estimate the error of the measurements (fig. S7).

Fabrication of the Tetrode Electrode

Each tetrode was built using two thin tungsten wires with a diameter of 20 μm and a length of 25 cm each. The wires were stuck together by running hands along them and then folded in half. The wires were hanged by the loop formed at one extremity and connected to a tetrode spinner (Neuralynx) from the other extremity. The four wires were twisted 130 turns forwards and then 15 turns backwards. Using a heat gun, the insulation of the tetrode was gently melted to increase its stiffness and the tightness of its tip (Magnification of the tetrode is shown in fig. S16B).

Data Analysis for Histology

All images were taken using fluorescence microscopy (EVOS FL Auto, Life Technologies, Grand Island, NY) (representative images are shown in fig. 1E) and analyzed with custom MATLAB scripts provided by Dr. Jeffrey Capadona of Case Western Reserve University (*50*). These scripts define the boundary of the hole created by the MiNDS increments from the hole boundary, up to 1100 μm away from the edge of the hole. For the purposes of data analysis, GFAP intensities were used as the primary indicator for the extent of glial scar formation around the implant. The intensities were then averaged into 50 μm bins, and normalized such that the intensity 900-1100 μm away was equal to 1. This was done for 4 pictures for each animal, which were averaged to create a GFAP intensity profile at different distances from the implant. The profiles for each of the four rats were then combined and averaged. The same procedure was applied to create Iba1 and NeuN profiles. All histological and confocal settings were kept

consistent across groups. Image contrast uniformly enhanced using ImageJ for visibility, such that 0.1% of pixels are saturated.

Histology Protocol for Chronic In Vivo Biocompatibility

The brain was embedded in frozen tissue embedding medium (Sakura Finetek), and frozen in a liquid nitrogen bath. 20 µm transverse slices were cut using a Leica CM1900 cryostat (Leica Biosystems Inc.), starting at the top of the brain, and descending 80 µm, past the tips of the previously implanted devices. Slides were stored at -80 ^{0}C. All histological sections that were analyzed were in planes along the shafts of the implants, approximately 4 mm from the top of brain, in the anterior pretectal nucleus. Slides were removed from the -80 ^{0}C freezer, placed at room temperature for 20 minutes, rehydrated by placing them in a 1x PBS solution for 10 minutes and then stained for glial fibrillary acidic protein (GFAP), microglia (Iba1), neurons (NeuN), and nuclei (Hoechst/DAPI). Samples were then immersed in a blocking solution (5% Bovine Serum Albumin (BSA)) for 50 minutes, followed by overnight incubation at 4 ^{0}C in a primary antibody incubation solution (1:100 mouse anti-GFAPx488 Alexafluor, 1:300 rabbit anti-NeuN, (EMD Millipore, Billerica, MA, USA), 1:300 goat anti-Iba1 in an incubation buffer (1% BSA, 1% normal donkey serum, 0.3% Triton X-100, 0.1% Sodium Azide).

Slides were rinsed 3 times in 1x PBS (0.1% Tween), and incubated in a secondary antibody solution (1:300 donkey x goat x Cy3 & 1:300 donkey x rabbit x Dy650 (Abcam) for 40 minutes. Samples were rinsed three times in 1x PBS, and incubated with a Hoechst solution (0.1 µg/ml) for 5 minutes, followed by mounting in a gold antifade reagent (Life Technologies, Carlsbad).

MiNDS Implantation in Rats

F344 (SAS Fischer) rats were purchased from Charles River Laboratories and maintained under standard 12 hours light/dark cycles. All materials used in surgeries were sterilized by autoclaving for 40 minutes at 250 ºF. Rats were anesthetized with isoflurane before having their heads shaven and disinfected with alternating povidone-iodine (Betadine) and 70% ethanol scrubs, three times each. Animals underwent bilateral craniotomy and had a MiNDS implanted on the left side of the cortex and a ground screw implanted on the right hand side (fig. S19). The screw was placed such that the tip of the MiNDS did not penetrate the brain. Briefly, the animals

were placed in a stereotactic frame, and a midline incision was made to expose the skull (figs. S19A-D). Then, two burr holes were created using a dental drill (fig. S19E). The left hand side burr hole was created using a 1 mm drill bit (Meisinger GmbH, Germany) and used for the MiNDS implantation, while the right hand side burr hole was made with a 0.5 mm drill bit and was used for the insertion of the ground reference screw. The ground screw was inserted 3 mm posterior to the bregma and 2 mm lateral to the midline (fig. S19F) while the MiNDS was implanted approximately 5 mm posterior to the bregma and 2 mm lateral to the midline until reaching a depth of 8.5 mm, targeting the substantia nigra as described on the Paxinos and Watson Rat Brain atlas (6 ed.) (fig. S19G). The MiNDS and screw were then cemented to the skull using C&B Metabond adhesive (Parkell Inc., Edgewood NY) and Orthojet dental cement (Lange Dental, Wheeling, IL USA) (figs. 19H,I), and the incision was closed using a 5-0 monofilament non-resorbable suture and 3M tissue glue (figs. S19J,K). Custom made caps composed of 31G stainless steel connector coated with UV-cured epoxy were inserted into the protruding PEEK tubing to prevent dust and microbes from entering the tubing causing clogging and infection. Animals were ambulatory and healthy 1-week post-op.

Five animals were euthanized at 8 weeks post-surgery and used for biocompatibility studies. The remaining animals were used for PET infusion studies.

High Pressure Liquid Chromatography (HPLC) Methods

To ensure that constituted muscimol (used for the chronic behavioral studies) pre-loaded into the pumps would remain active throughout the time implanted within the animal, a sample of the muscimol solution was stored in an incubator at 37°C and HPLC assays were used to verify the stability of muscimol over 8 serial dilutions at 0.2, 0.1, 0.05, 0.025, 0.0125, 0.00625 and 0.003125 mg/ml at different time points for 50 days (fig. S21). This was done according to previously described protocols for HPLC characterization of muscimol (*51*). HPLC assays were performed on an Agilent 1200 series system with a 25 cm (L) x 4.6 mm (ID) Spherisorb ODS-2 column (Waters, Millford), containing 5 µm silica particles and 80A pore size. The column was eluted with an aqueous solution of 0.5% v/v HBTA (heptafluorobutyric acid, Sigma Aldrich) at 1 ml/minute. Then, 20 µl of samples were injected into the column and muscimol was detected using a UV detector with the absorbance wavelength set at 230 nm, and reference wavelength set

at 360 nm. Muscimol concentration was determined by comparing the area under the curve at the appropriate retention time (5.5 minutes) to a calibration curve of known concentrations.

Non-Invasive Brain Imaging Using Positron Emission Tomography (PET)

Radioactive Cu-64 was obtained from the Mallinckrodt Institute of Radiology (St. Louis, MO) in the form of Copper Chloride, and diluted with saline to 3 µCi/µl activity concentration. A Cu-64 solution was then infused intracerebrally into F344 Fischer Rats (Charles River Laboratories) using each of the following four methods:

(i) A 10 µl luer lock syringe (#1701 Hamilton, Reno, NV) was connected to a 31G needle and pre-loaded with 5 ml of Cu-64 solution. A 1 mm burr hole was created in an untreated animal under isofluorane anesthesia 5 mm posterior to the bregma and 2 mm lateral from the midline (identical to MiNDS surgical procedure shown in fig. S19. The needle was lowered stereotaxically through the burr hole, 8 mm into the brain. 2 µl of Cu-64 was delivered using a Stoelting Quintessential Stereotaxic Injector, at a rate of 0.2 µl/minute for 10 minutes. The needle was left in place for 5 minutes post end-infusion before being retracted slowly. The burr hole was then covered with bone wax and the cranial incision sutured with 5-0 non-resorbable monofilament suture. This protocol was used as an acute infusion case control, where the cannula was inserted only for the duration of the infusion and not chronically implanted.

(ii) Animals with an implanted MiNDS were anesthetized with isofluorane. One of the fluidic outputs of the device was connected to the same syringe/needle set up previously described in case (i). 1.67 µl of Cu-64 was delivered at a rate of 10 µl/hour for 10 minutes. In another trial, 667 nl of Cu-64 was delivered at a rate of 10 µl/hour for 4 minutes

(iii) Animals with an implanted MiNDS were anesthetized with isofluorane. One of the fluidic outlets of the MiNDS was connected to an iPrecio pump. As in case (ii), one of two infusions were done: (1) 1.67 µl of Cu-64 was delivered at a rate of 10 µl/hour for 10 minutes, or (2) 667 nl of Cu-64 was delivered at a rate of 10 µl/hour for 4 minutes.

(iv) Agarose gel (0.6% by weight) had a MiNDS implanted. This case is used as a control due to the similarity in mechanical properties to the brain tissue (*52*). As in case (ii), one of the fluidic outputs of the device was connected to the same syringe/needle set up previously described. One of two infusions were done: (1) 1.67 µl of Cu-64 was delivered at a rate of 10 µl/hr for 10 minutes, or (2) 667 nl of Cu-64 was delivered at a rate of 10 µl/hour for 4 minutes.

Immediately following the incision suture, in case (i) the anesthesized animal was imaged using a Perkin Elmer G8 PET /CT Preclinical Scanner for six 10 minutes frames over the course of 30 minutes. In cases (ii), (iii) & (iv) the anesthesized animal ((ii) & (iii)) or agarose phantom (iv) was imaged using a Perkin Elmer G8 PET /CT Preclinical Scanner for five 5 minutes frames over the course of 20 minutes. Imaging began prior to infusion, through infusion, and up to 5 mins post-end infusion. Images are reconstructed using MLEM 3D with 60 iterations. Representative maximum intensity slices and intensity vs. position curves are shown in figs. S12E-F,S13F-H.

Only PET could be performed on the entire animal, due to the size of the bore and gantry. For case (i), computed tomography (CT) was performed as well: the animal was euthanized using CO_2 asphyxiation and decapitated. The head was then imaged with PET and CT for a single 10 mins frame. Co-registration was then done with the original PET Data that was obtained in vivo and the PET/CT data that was obtained ex-vivo. A representative 3D image with both CT and PET is shown in fig. S14.

PET data was then analyzed in VivoQuant Analysis software (inviCRO, LLC, MA, USA) by using 2 methods: (1) by creating a 3D region of interest (ROI) around the infused bolus, and (2) by drawing a line profile horizontally across the maximum intensity plane of the bolus. The ROI was generated using connected thresholding techniques whereby the edges were defined by an intensity value equal to 10% the peak intensity at the center, I, for a total width, w (Fig. 2G). The summed intensity within the ROI was then calculated for each frame, and the results linearly normalized such that the maximum intensity value for each infusion case was equal to 1. The line profile analysis illustrated the diffusion behavior of the bolus over time (figs. S12A,B,S13A,B). Here, the total signal within ROI at a time point is the summed signal detected over the 5 minutes exposure time of each scan.

Acute Recording for Tetrode MiNDS Study

Adult female rats (F344) were anesthetized by exposure to isoflurane (2%, mixed with oxygen) and mounted in a stereotactic frame. A craniotomy was performed 2.5 mm posterior and 2.5 mm lateral to the bregma. A second craniotomy for the reference electrode was conducted 2.5 mm anterior to the bregma. A millmax pin was inserted into the brain to serve as the reference electrode. MiNDSs prepared with a tungsten tetrode as the electrode component were

connected to an electrode interface board (Neuralynx) which in turn interfaced to a computer via an Intan RHD 2000 USB interface board (Intan Technologies).

The dura was removed and the device was lowered into the brain to a depth of 2.5 mm and a location with unit activity was identified (fig. S17). The local neural signals were recorded with Open Ephys GUI software. Prior to drug infusion, the local signals were recorded for 30 minutes to ensure stable spikes were located. After the baseline recording, 150 nl of saline were infused into the site at a flow rate of 100 nl/minute and the activity was recorded for another 30 minutes. Local silencing was achieved by the infusion of muscimol (1.0 mg/ml) via the other device channel (150 nl, 100 nl/minute). Recording was continued for additional 30 minutes post muscimol infusion. Saline washout was then performed by infusing 1.0 µl of saline at a flowrate of 100 nl/minute and the activity was monitored until recovery.

Behavioral Studies

A custom-made circular acrylic dish 1 foot in diameter and 3 feet in height was placed in an opaque black box (fig. S22). A GigE digital camera (resolution 750 x 480 pixels, The Imaging Source) was held in a stand such that it was directly above the dish, with the entire dish being in the field of view. The camera was connected to a computer where videos were acquired using IC Capture (The Imaging Source) and then imported into Ethovision software (Noldus) for further analysis. A rat was implanted with the MiNDS and two pumps pre-loaded and flushed with either saline or muscimol, as described above. The animal was placed within the dish and recorded over the course of 5 hours. During the first 1 hour, no infusion was set. This was to establish a baseline recording of the animal's regular behavior. Then, Pump A infused 1.67 µl of saline for 10 minutes. After 1 hour, Pump B infused an identical 1.67 µl of muscimol (concentration 0.2 mg/ml) for 10 minutes. The animal was further imaged for 3 hours after the second infusion before being returned to its home cage. All experiments were done during the light hours of the animal's 12 hours dark-light cycle. Videos were imported into Ethovision, where they were analyzed for ipsilateral and contralateral rotations over time. A rotation was defined as a 180° turn of the Center-Nose vector.

Selective Chemical Modulation in Awake Nonhuman Primate (NHP)
Device and Infusion Preparation Procedures

Solutions used for infusion through the MiNDS were aCSF (artificial cerebrospinal fluid, Tocris Biosciences) and muscimol (2 mg/ml in aCSF, Sigma-Aldrich). The MiNDS and guide cannula were sonicated in a detergent solution (Alconox, Inc.), rinsed with water, and then sonicated and soaked in 70% ethanol followed by water until they were ready for implantation. Radel (Idex-HS) fluidic tubing and fittings were similarly cleaned. A Harvard 33 Twin Syringe Pump and microliter syringes (Model 702 RN SYR, Hamilton Co.) were used for all infusion procedures. Prior to loading targeted solutions into the MiNDS, the cannulae were infused with 70% ethanol at 200 nl/minute followed by water at 200 nl/minute. The aCSF and muscimol solutions were individually backfilled into the two different tubing (prefilled with mineral oil) at a rate of 2 µl/minute prior to being connected to the MiNDS ports. The targeted solutions were then infused through the MiNDS cannula at a rate of 100 nl/minute for 30 minutes to ensure sufficient permeation.

NHP Surgery

One rhesus monkey (6.5 kg female) (*Macaca mulatta*) was used. All experimental procedures were in accordance with the Institute Animal Care and Use Committee, followed guidelines of the MIT Committee on Animal Care, and complied with Public Health Service Policy on the humane care and use of laboratory animals. The monkey had been adapted to transitions from cages to a primate chair using pole-and-collar and food reinforcement. Experiments took place in a dark and electrically isolated chamber designed for NHP studies. The monkey had already been fitted with a chronic chamber and grid for electrode mapping, as described in (*49*). For the pilot studies reported here, the monkey received a chamber aimed at the cortex and the striatum in the right hemisphere and placed at an angle of 4° in the coronal plane for chronic recording under aseptic conditions and Sevofluorane anesthesia. Precise anatomical targeting was achieved by structural MRI (3 Tesla) to measure relative grid-hole coordinates. For the infusion and recording in primate, the MiNDSs were introduced into a chronically implanted guide tube or acutely introduced guide tube onto the chamber grid to target a structure and perform recording. The recording was performed after surgery.

Recording and Infusion Procedures for NHP Study

A micromanipulator (Narishige, MO-97A) was used to slowly lower the MiNDS after penetrating the dura matter using a 26G guide tube (ConnHypo, 26G-XTW) (Fig. 4A). The tip of the MiNDS was lowered into the cortex, or at targeted coordinates of anterior posterior, AP +23 mm (relative to interaural line) and mediolateral, ML +2 mm as estimated by grid holes that had been aligned to coronal MRI images (Fig. 4B).

Electrophysiological recording of spikes and local field potential was performed through Cheetah recording system (Neuralynx) using an HS-27 headstage. The reference and ground electrodes were low-impedance (< 1 kOhm) 75 µm diameter tungsten electrodes placed inside the granulation tissue above the skull. Data were collected at a sampling rate of 32,556 samples/s with bandpass cut off frequencies at 0.5 Hz and 9000 Hz. For spike detection and sorting, data were high pass filtered at 300 Hz.

Spike Sorting

Electrophysiological data were processed offline in Offline Sorter (Plexon) to identify single unit activity and in neurophysiological data analysis software (Neuroexplorer) to create rate histograms based on these detected units. To identify individual units, the amplitude threshold for the highpass filtered data was set at 17 µV and sorted based on principle component analysis algorithms in Offline Sorter (T-Distribution Expectation Maximization) as well as user-input box templates to select expected ranges for peak and post-hyperpolarization waveforms. Waveforms for each period (baseline, aCSF infusion and post-infusion, muscimol infusion and post-infusion) were grouped to generate mean and standard deviations of the unit waveform over time.

Data Analysis for Recorded Local Field Potential

For analysis of recorded local field potentials in primate (fig. S25), recorded signals were first downsampled to an effective sampling rate of 1 kHz. All analyses were performed in Matlab. Signals were analyzed in windowed periods of 700 ms with no overlap. Periods with large amplitude fluctuations (due to movement or other sources of noise) were removed by detecting signals greater than 0.15 mV in magnitude. Power spectra were generated by generating fast fourier transform averaged over clean 700 ms periods of LFP squared (i.e.,

power) from a 10 minutes interval to display changes in gross LFP power over the course of infusions and between these infusions. Spectra were computed using a single taper with a time bandwidth product of 1.8 (*53*). Significance boundaries were set using a p level of 0.05 and these boundaries are displayed by the two curves generated for each spectrum for each 10 minutes time period. A pink noise spectrum was log-fit to the baseline LFP power (first 10 minute of recording before any infusion) using $p = af b$, where f indicates frequency, and the parameters a and b were fitted to the power averaged over this period. This pink-fit power was then removed from all generated spectra to improve visualization of the relevant changes at a broad range of frequencies. Power fluctuations across the 10 minutes periods are displayed as relative changes in log-scale (dB) to the baseline ('-10 minutes' labeled curve).
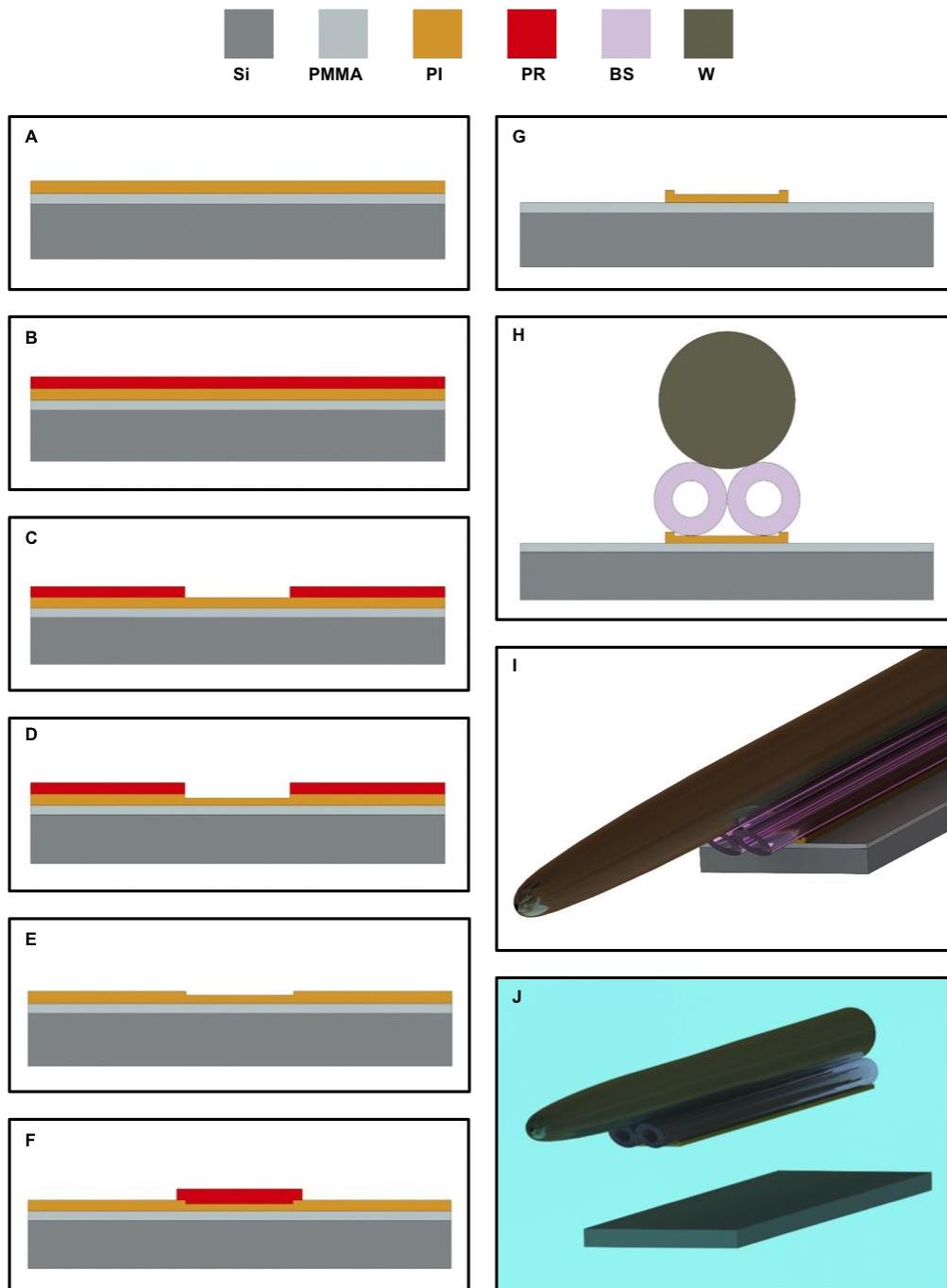
Fig. S1. Schematic illustration of fabricating a MiNDS. Cross sectional illustration of (**A**) the stack of temporary substrate, Si/sacrificial layer, PMMA/PI, (**B**) photoresist layer on stack in (A), (**C**) photoresist pattern for etching the underlying layer of PI to define the trench of the PI template, (**D**) selective etching PI layer, (**E**) removing photoresist, (**F**) photoresist pattern for etching the underlying layer of PI to define the PI template, (**G**) the structure of the PI template,

(H) aligning of BSs and W electrode on the PI template. **(I)** Angled view of the structure in (H). **(J)** Dissolving PMMA layer in acetone bath to retrieve the MiNDS components from the temporary substrate, Si.
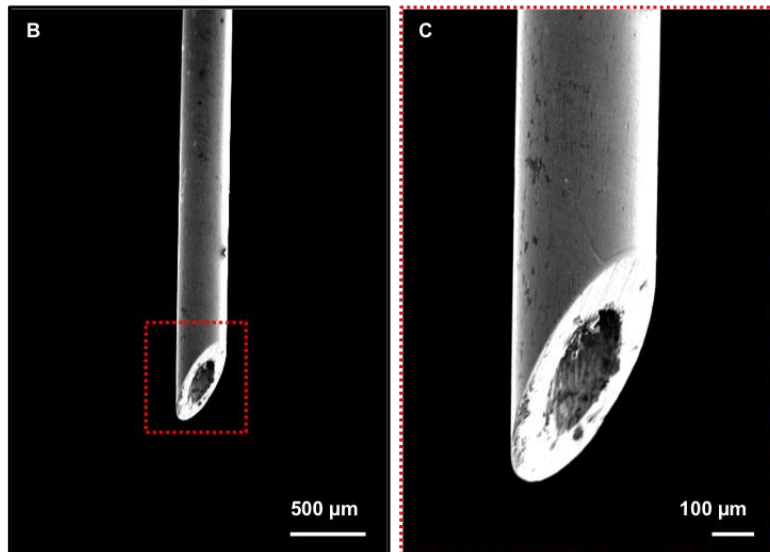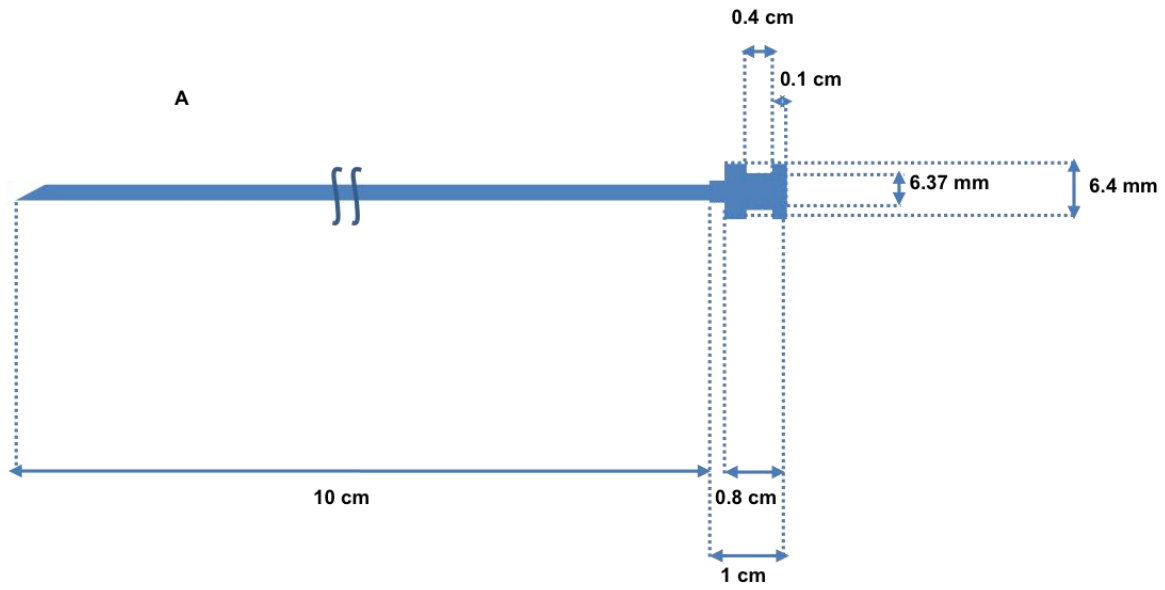
Fig. S2. Schematic illustration and SEM image of Hamilton needle. **(A)** Schematic illustration of the Hamilton needle. **(B)** SEM image of a Hamilton needle with 30° tip angle. **(C)** Magnified view of red dashed box in (B).

Fig. S3. Photographs of the steps for polishing and cleaning the tip of a BS channel. (A)
Image of a BS channel polishing procedure to 30⁰ tip-angle with Ultrapol End & Edge. **(B)** The
magnified view of the holder (red box) in (A). **(C)** Image of a BS channel attached in the holder.
(D) Picture of an ultrasonic cleaner with beaker used for cleaning BS residues after polishing.
(E) Picture illustrating the cleaning procedure of the BS after polishing.
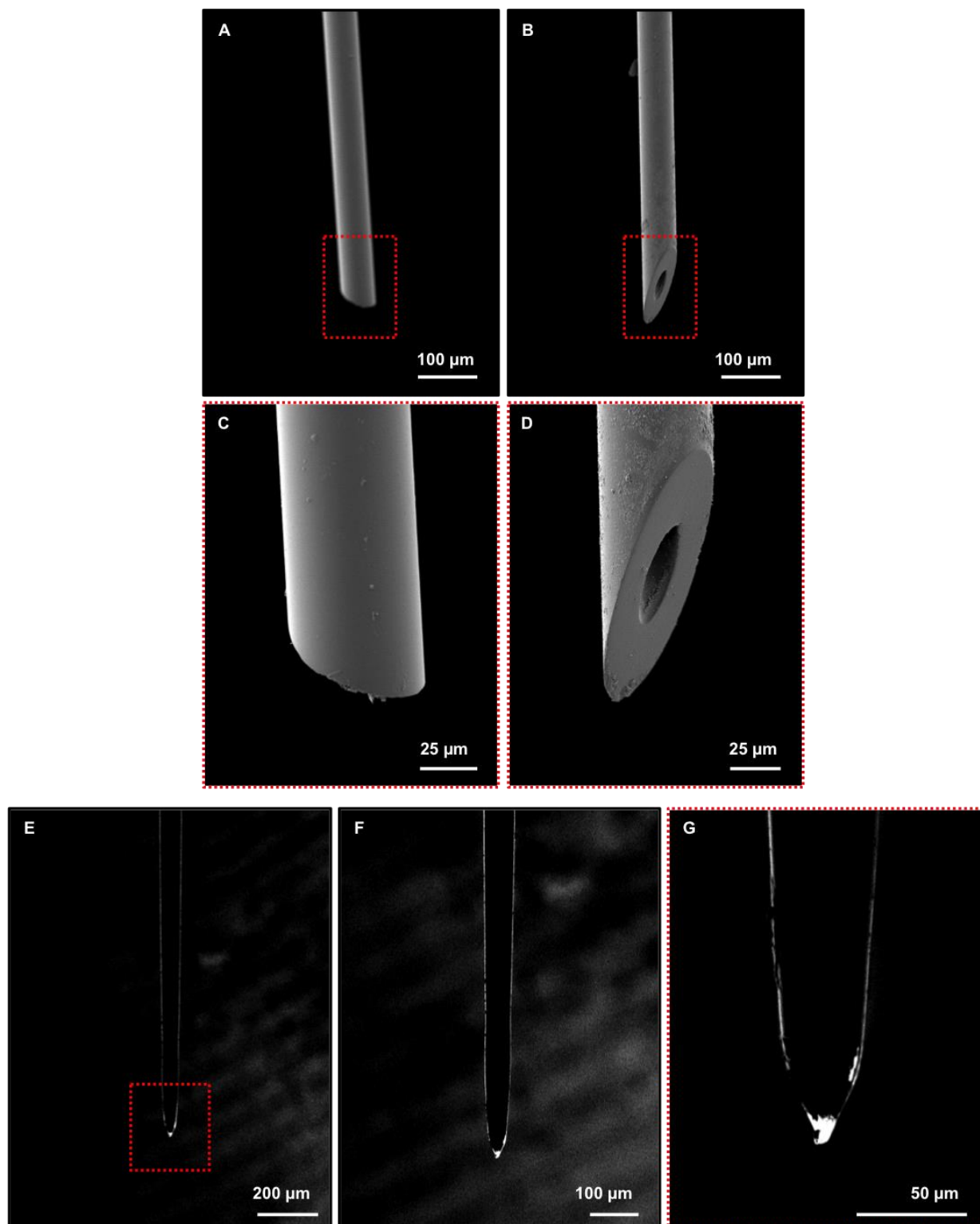
Fig. S4. SEM images of the components of a MiNDS. SEM images of **(A)** unpolished and **(B)** polished BS channel. **(C, D)** Magnified views of the tip of BS channel identified by the red dashed box in (A) and (B), respectively. **(E)** SEM image of the tungsten electrode. **(F, G)** Magnified SEM images of the tip of the electrode identified by the red dashed box in (E).
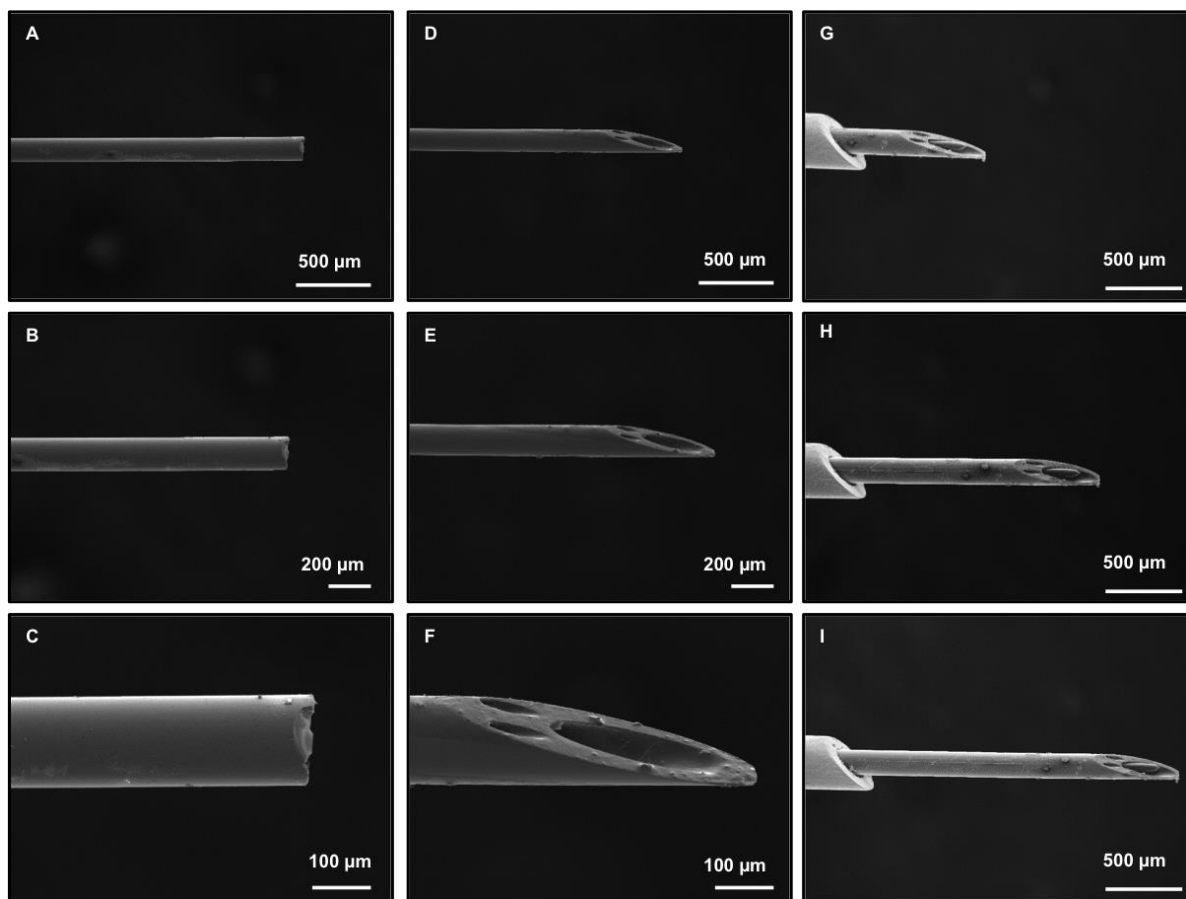
Fig. S5. SEM images of the components of a BS tip aligner. SEM images of **(A, B, C)** unpolished and **(D, E, F)** polished BS aligner tip with various magnifications. SEM images of a MiNDS with a length of **(G)** 0.8 mm, **(H)** 1.5 mm, and **(I)** 2.0 mm BS aligner tip.
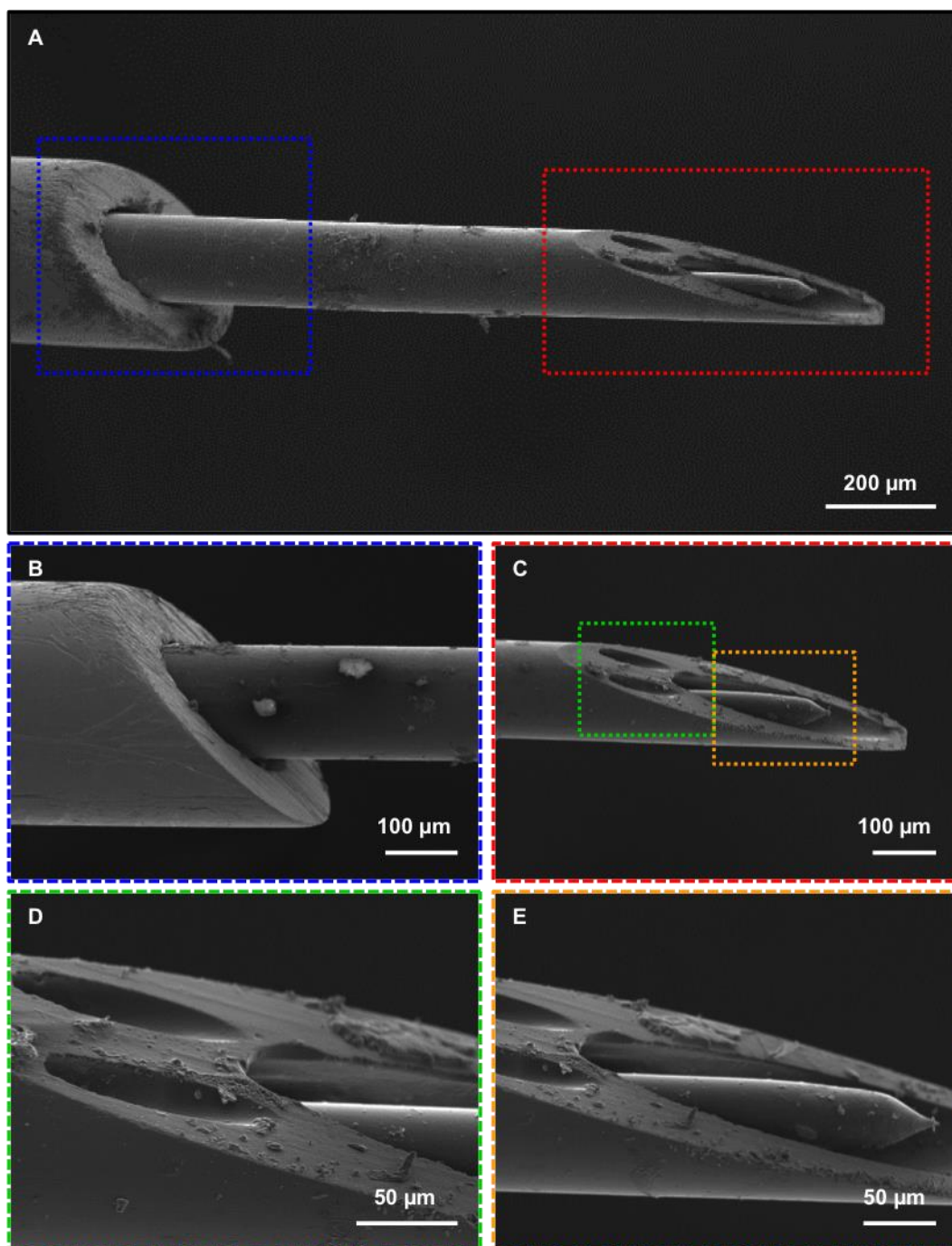
Fig. S6. SEM images of a completed MiNDS. (A) SEM image of a MiNDS, consisting of tungsten electrode and BS channels. **(B, C)** Magnified SEM images of blue and red dashed boxes in (A) respectively. **(D, E)** Magnified SEM image of BS channel (green) and tungsten electrode (orange dashed box) in (C) respectively.
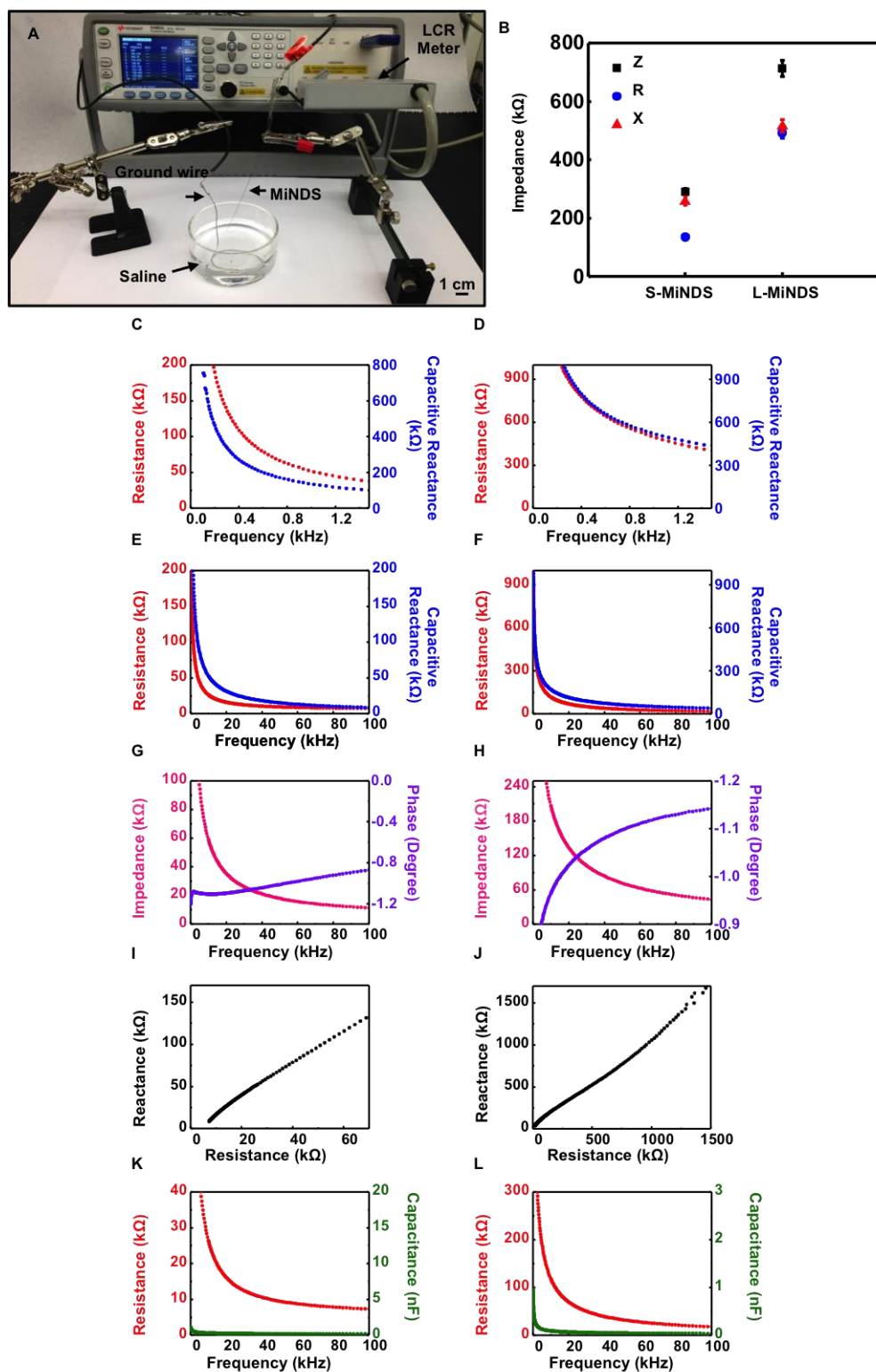
Fig. S7. The electrical characterization of S- and L-MiNDS at 37°C in saline. (A) The experimental setup of impedance measurement for W electrode. **(B)** Impedance vs time graphs for S-MiNDS and L-MiNDS; where r: Resistance, x: Reactance and z: Impedance **(C, D)**

Resistance-capacitive reactance vs. frequency graphs at high frequency for S-MiNDS (C) and L-MiNDS (D). **(E, F)** Resistance-capacitive reactance vs. frequency graphs at low frequency for S-MiNDS (E) and L-MiNDS (F). **(G, H)** Impedance-phase (degree) vs. frequency graphs for S-MiNDS (G) and L-MiNDS (H). **(I, J)** Reactance vs. resistance graphs for S-MiNDS (I) and L-MiNDS (J). **(K, L)** Resistance-capacitance vs. frequency graphs for S-MiNDS (K) and L-MiNDS (L).
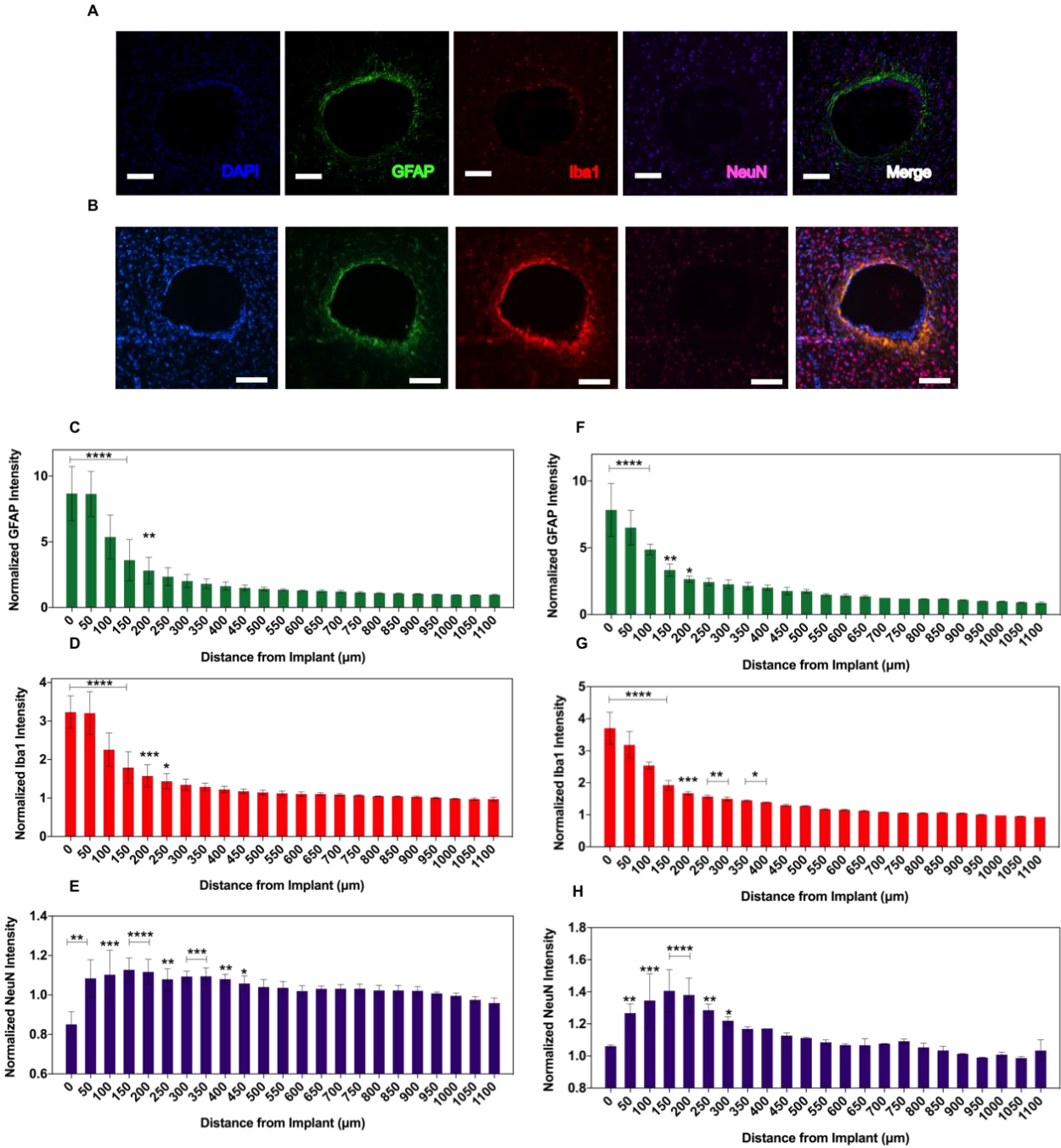
Fig. S8. Chronic in vivo biocompatibility assessment. (A) Representative immunohistochemical staining of a single brain section for DNA (DAPI, blue), astrocytes (GFAP, green), activated microglia (Iba1, red), and neurons (NeuN, purple) in a horizontal brain slice around the stab wound created by implanted MiNDS shank, 8 weeks after MiNDS implantation. **(B)** Representative immunohistochemical staining for DNA (DAPI, blue), astrocytes (GFAP, green), activated microglia (Iba1, red), and neurons (NeuN, purple) in a horizontal brain slice around the stab wound at the tip of the MiNDS, 8 weeks after MiNDS

implantation. Scale bars, 100 µm. **(C)** GFAP, **(D)** Iba1, and **(E)** NeuN expression intensity as a function of distance away from the edge of the stab wound at the MiNDS shank measured 8 weeks after MiNDS implantation. **(F)** GFAP, **(G)** Iba1, and **(H)** NeuN expression intensity as a function of distance away from the edge of the stab wound at the device tip measured 8 weeks after MiNDS implantation. Stain intensity was quantified in 2 µm radial increments from stab wound perimeter, up to 1100 µm away. Results are normalized to intensity 900-1100 µm away, and averaged into 50 µm bins. The calculated error bars are the standard errors (n=5 rats, 20 slides). (For all graphs: *p<0.05, **p<0.01, ***p<0.005, ****p<0.001). Statistical analysis was done using one-way ANOVA followed by Dunnett test.
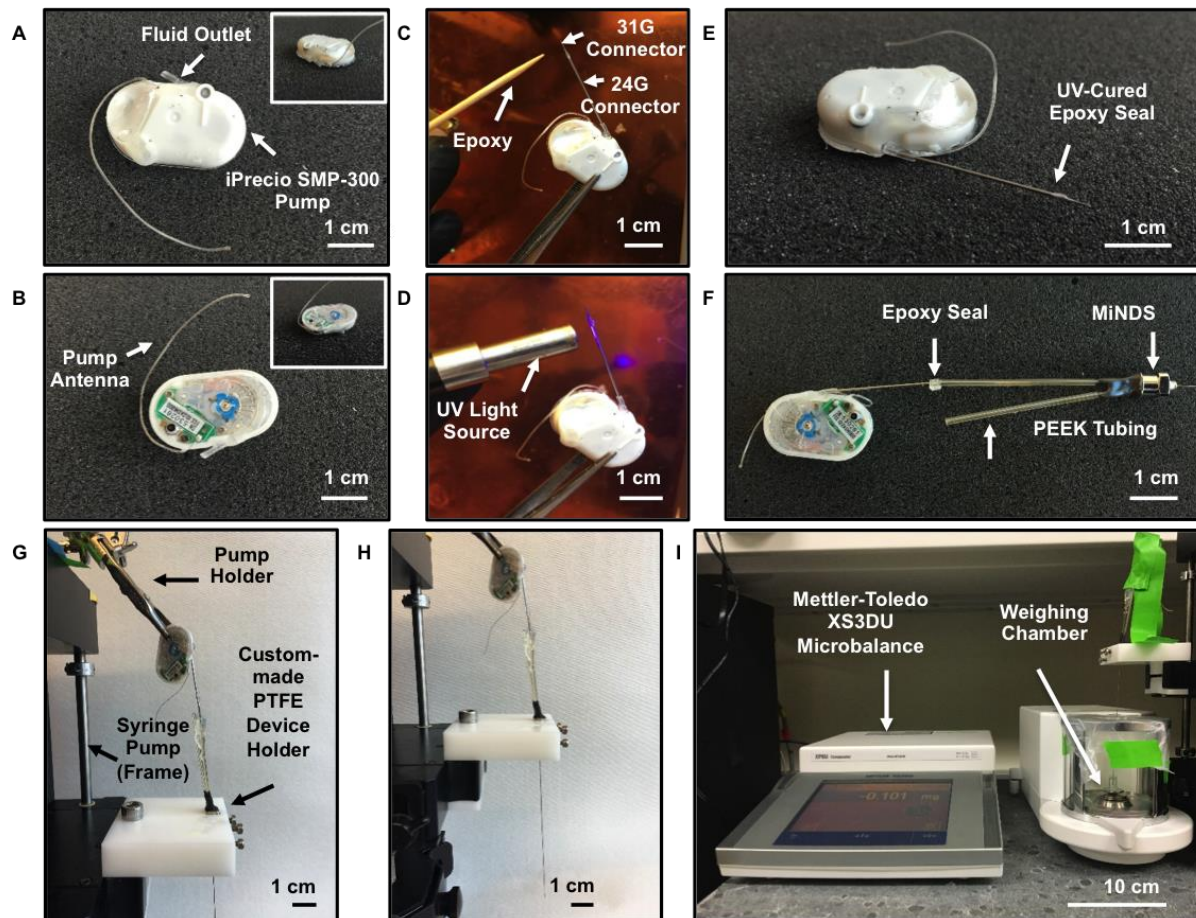
Fig. S9. Pump characterization setup. (**A**) Top and (**B**) Bottom images of an iPrecio pump with original external tubing cut, leaving only the first 2.5 mm of outlet tubing. (Right inset images of (A) and (B) show isometric views of top and bottom of the SMP-300 pump, respectively). (**C**) A 24G stainless steel connector is inserted into the pump fluid outlet and a 31G connector placed within the larger connector. (**D**) The 24G and 31G are glued together using UV light curable epoxy, creating a water-tight secure junction. (**E, F**) The protruding end of the 31G connector is inserted into the PEEK tubing of the MiNDS and the junction glued using the same UV light curable epoxy. (**G, H**) The MiNDS is placed into a custom-made PTFE (polytetrafluoroethylene) holder attachable to a syringe pump to be used as a vertical frame (Harvard Apparatus PHD 2000), and (**I**) the assembly combined with a Mettler Toledo microbalance for pump characterization experiments.
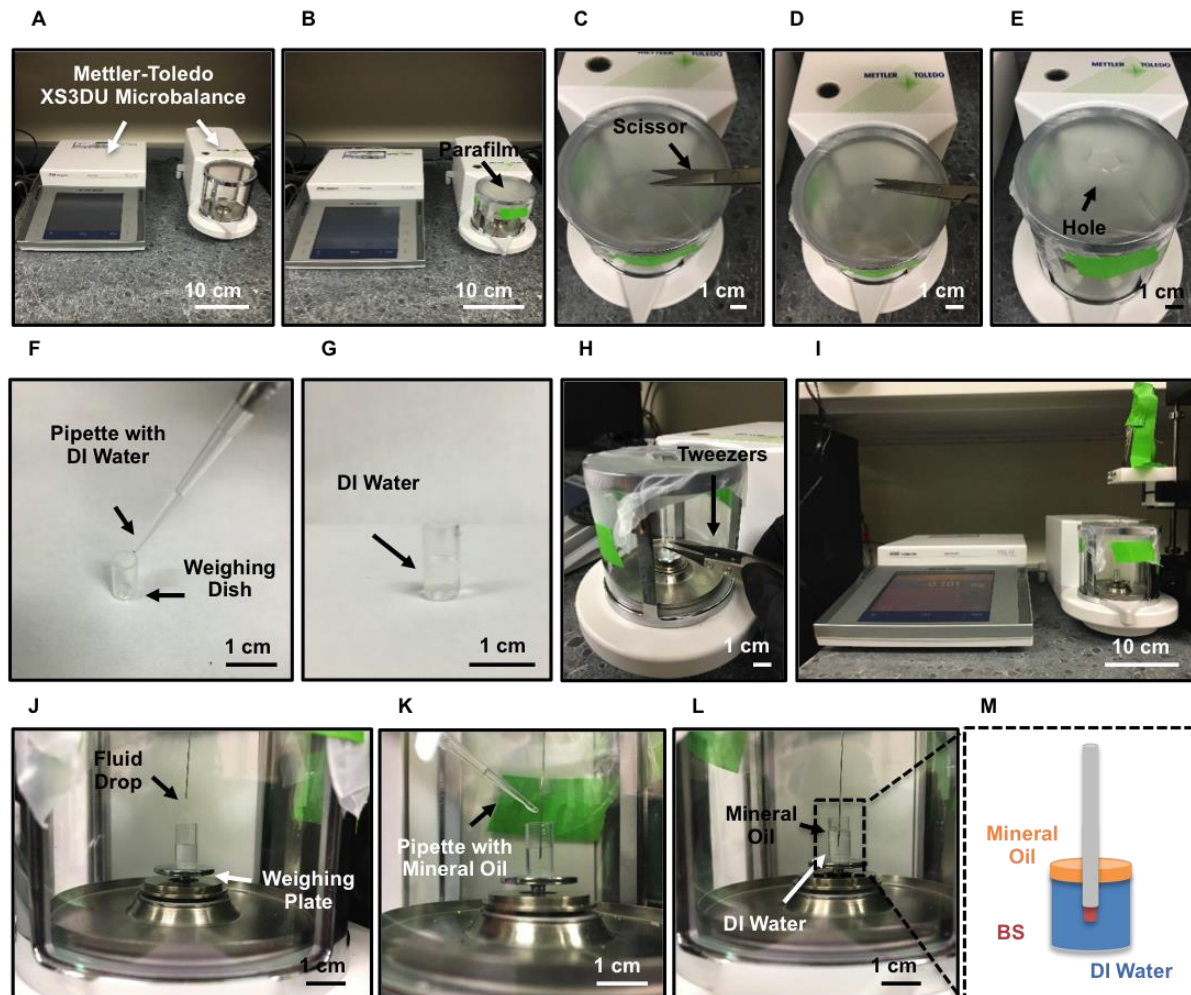
Fig. S10. Pump characterization protocol. (**A**) A Mettler Toledo Microbalance is used, with sensitivity set to 1 µg. (**B**) The glass cap of the weighing chamber is removed and replaced with parafilm stretched tightly around the edges. (**C, D**) The parafilm is cut in the center, and (**E**) a small round hole is made. (**F, G**) The weighing cup is filled with 30 µl of DI water, and (**H**) placed in the weighing chamber. (**I**) The assembled MiNDS-pump setup is lowered into the chamber, and flushed. (**K**) Once liquid is seen protruding from the edge of the device, it is lowered into the chamber, such that the tip is submerged within the water. A thin film of mineral oil is then placed on top of the water (**L**), to prevent evaporation from interfering with the recorded weights. (**M**) A diagram illustrates the distinct layers of water and oil in the weighing dish, and relative position of the MiNDS tip.
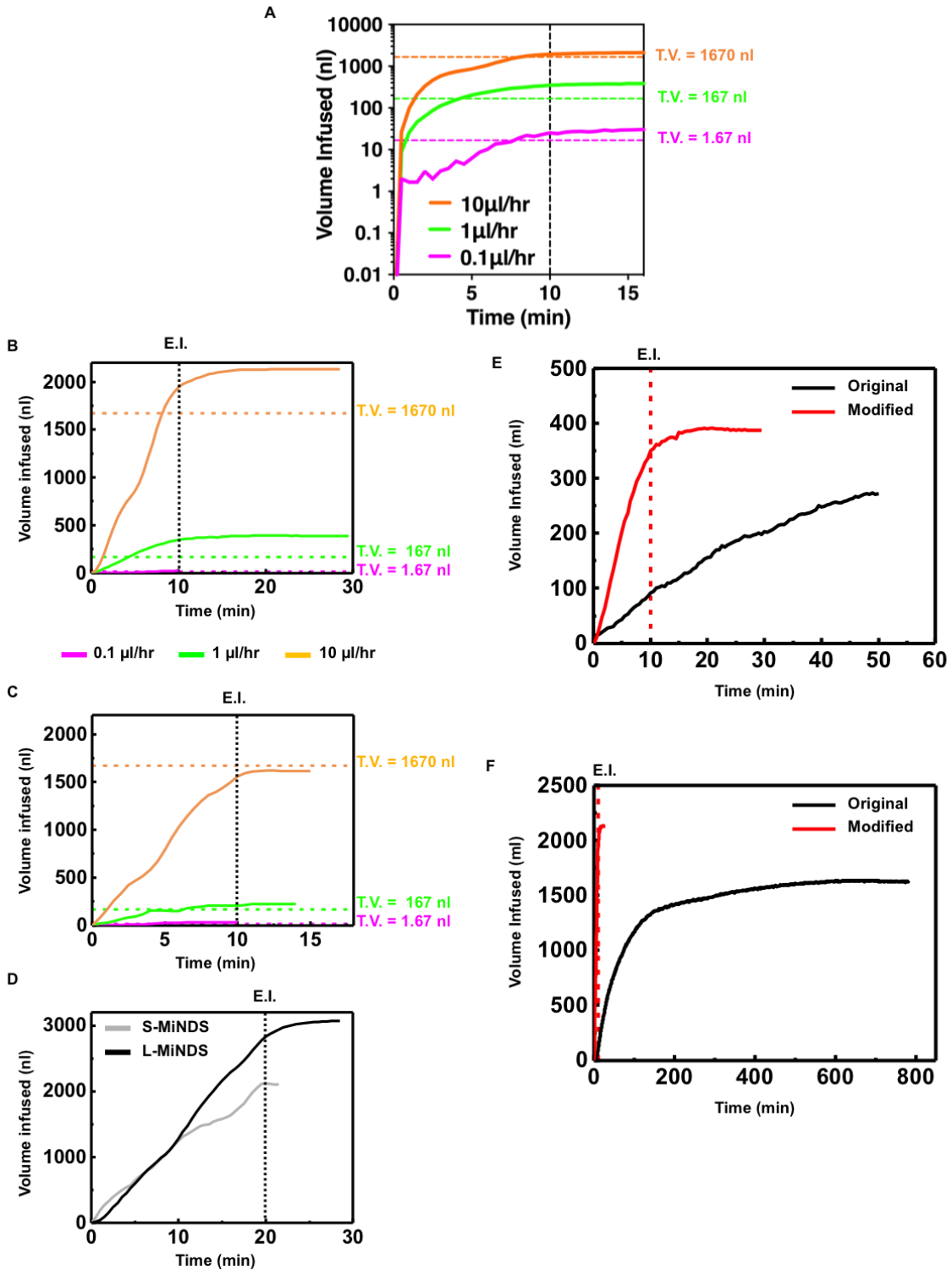
Fig. S11. Infusion profiles of the iPrecio pump. (A) Mean infusion profiles of the iPrecio pump through the L-MiNDS (n=4 infusions per profiles). Three 10 minutes infusions each at a

different profile are shown: 10 μl/hour, 1 μl/hour, 0.1 μl/hour. E.I and T.V. represent the end of infusion and theoretical value of volume infused, respectively. **(B, C)** Mean infusion profiles over time for the iPrecio pumps through the **(B)** L- and **(C)** S-MiNDS. For each, three 10 minutes protocols were tested, each at a different flow rate: 10 μl/hour, 1 μl/hour, 0.1 μl/hour. **(D)** The mean infusion profile for a 20 minutes infusion at 6 μl/hour, through both S- and L-MiNDSs. E.I and T.V. represent the end of infusion and theoretical value of volume infused, respectively. **(E, F)** Mean infusion profiles over time for original and modified iPrecio pumps through L-MiNDS. Two 10 minutes infusions each at a different flow rate are shown: **(E)** 1 μl/hour and **(F)** 10 μl/hour. For S-MiNDS infusion profile in **(D)**, n=3. For original pump infusion profile in **(F)**, n=1. For all other graphs, n=4.

A Syringe pump in agarose — t = 5 min, t = 10 min, t = 15 min, t = 20 min — 0.5 mm, 2 mm

B Syringe pump in brain

C iPrecio pump in brain

9e+06 / 4e+06 / 3e+06 / 0 (blue scale)
5e+05 / 4e+05 / 2e+05 / 0 (green scale)
5e+06 / 3e+06 / 1.5e+06 / 0 (red scale)

Becquerel/ml

D

The Trials	Bolus Volume ± Standard Deviation (mm³)
Syringe pump in agarose	3.78 ± 2.43
Syringe pump in brain	4.64 ± 1.43
iPrecio pump in brain	4.36 ± 0.45

E (Normalized Intensity vs Position (mm)) — 5 min, 10 min, 15 min, 20 min
F — 5 min, 10 min, 15 min, 20 min
G — 5 min, 10 min, 15 min, 20 min

Position (mm)

H Normalized ROI Sum Intensity

Time (min)	iPrecio			Syringe Pump			Agarose		
0	0.0000	0.0000	0.0000	0.0000	0.0000	0.0000	0.0000	0.0000	0.0000	0.0000
5	0.0490	0.9847	0.1165	0.1102	0.1108	0.1025	0.3898	0.0623	0.2179	0.6532
10	0.4280	0.9310	0.9385	0.9714	0.5488	1.0000	0.6208	0.9860	0.7818	1.0000
15	0.9689	0.9080	0.9846	1.0000	0.7069	0.8852	0.6993	1.0000	1.0000	0.5934
20	1.0000	0.8773	0.9808	0.9143	0.8056	0.9262	1.0000	0.7814	0.6196	0.4059

Fig. S12. Large infusion characterization via PET. (A-C) Time sequence of PET images acquired at 5, 10, 15, and 20 minutes after radioactive Cu-64 infusion. Radiaoctive Cu-64 (3 µCi/µl, 10 minutes infusion at 10 µl/hour, 1.67 µl total volume infused) was infused through (**A**) S-MiNDS embedded in agarose (0.6% by weight) using a syringe pump, (**B**) S-MiNDS implanted in a rat using a syringe pump, or (**C**) S-MiNDS implanted in a rat using iPrecio

pumps. T= 0 minute represents onset of acquisition and infusion. Fluorescence intensity scale is shown on the right for the three conditions tested. (**D**) Bolus Volume calculated using 3D ROI from center of bolus to edge (defined as 10% of peak intensity) (n=3). (**E-G**) Normalized intensity in relation to position curves at 5, 10, 15 and 20 minutes from the beginning of Cu-64 infusions (3 µCi/µl, 1.67 µl infusion at 10 µl/hour) delivered into (**E**) an agarose phantom using a syringe pump, in rat brain through implanted S-MiNDS using (**F**) a syringe pump, and (**G**) an iPrecio pump. (**H**) Normalized ROI sum intensity table shown in Fig. 2F.

D
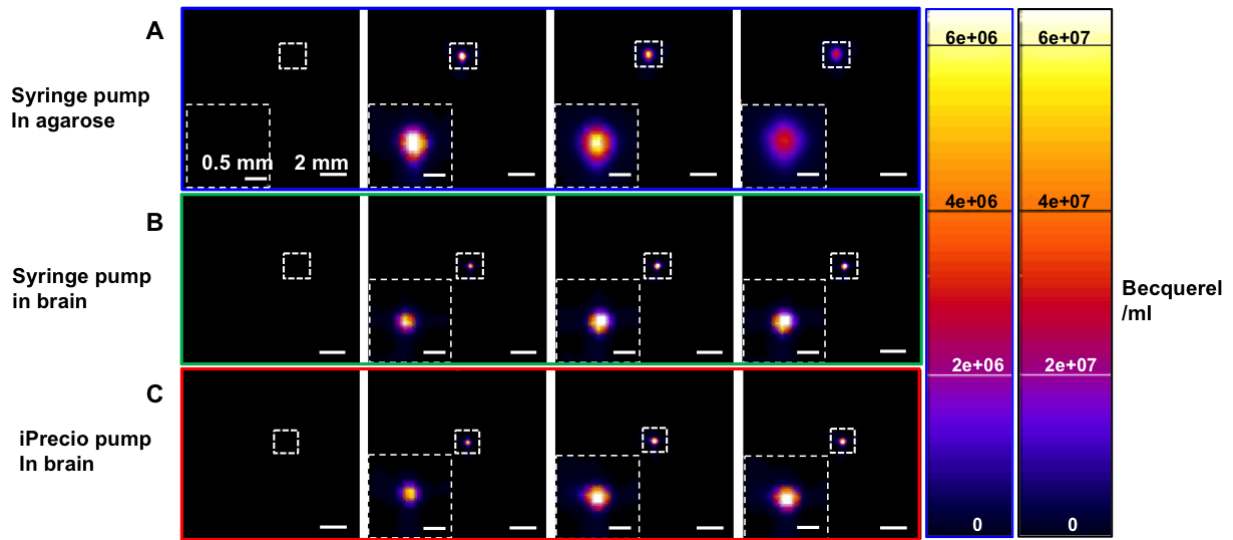
The Trials	Bolus Volume ± Standard Deviation (mm³)
Syringe pump in agarose	2.35 ± 1.14
Syringe pump in brain	1.81 ± 0
iPrecio pump in brain	2.80 ± 0.15
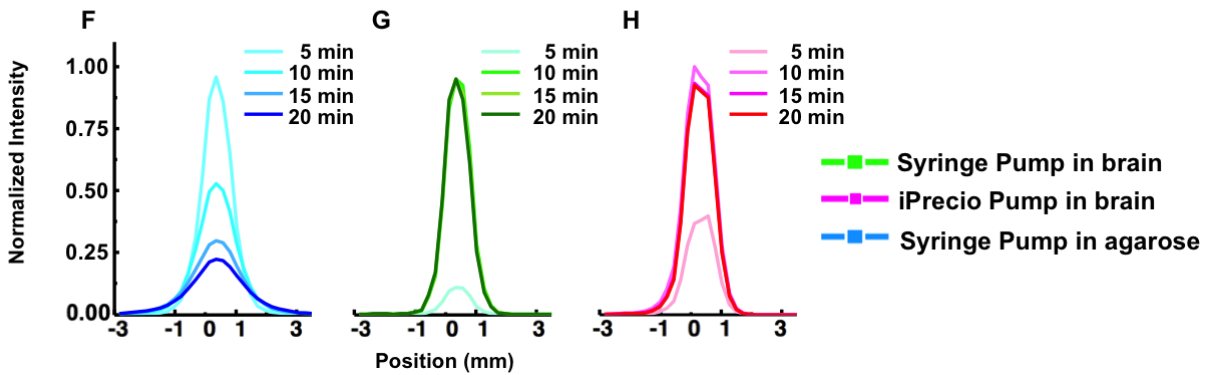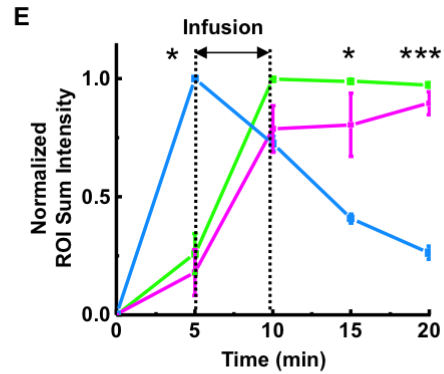
I

Normalized ROI Sum Intensity

Time (min)	iPrecio			Syringe Pump				Agarose		
0	0.0000	0.0000	0.0000	0.0000	0.0000	0.0000	0.0000	0.0000	0.0000	0.0000
5	0.1500	0.3848	0.0000	0.1236	0.4511	0.2003	0.4695	1.0000	1.0000	1.0000
10	0.7500	1.0000	0.6124	1.0000	0.9903	1.0000	0.9997	0.6757	0.7006	0.7970
15	0.5000	0.9120	1.0000	0.9842	1.0000	0.9829	1.0000	0.3615	0.4271	0.4334
20	1.0000	0.8720	0.8140	0.9709	0.9903	0.9565	0.9944	0.2790	0.3056	0.2012

Fig. S13. Small infusion characterization via PET. (A-C) Time sequence of PET images acquired at 5, 10, 15, and 20 minutes after beginning of radioactive Cu-64 infusion. Radiaoctive Cu-64 (30 µCi/µl, 4 minutes infusion at 10 µl/hour, 667 nl total volume infused) was infused through (**A**) S-MiNDS embedded in agarose (0.6% by wt.) using a syringe pump, (**B**) S-MiNDS implanted in a rat using a syringe pump, or (**C**) S-MiNDS implanted in a rat using iPrecio pumps. Fluorescence intensity scale is shown on the right for the three conditions tested (**D**) Bolus Volume calculated using 3D ROI from center of bolus to edge (defined as 10% of peak intensity) (n=3). (**E**) Normalized ROI sum intensity derived from PET images as function of time profile of Cu-64 infusions (30 µCi/µl, 4 minutes infusion at 10 µl/hour, 667 nl total volume infused) delivered into an agarose phantom (0.9% by weight), and in the rat brain through implanted S-MiNDSs using a syringe pump and an iPrecio pump. (n=3 trials; error bars represent standard error). Statistical analysis was done using one-way ANOVA followed by Tukey test *p<0.0332, ***p<0.0002). (**F-H**) Normalized intensity as function of position curves at 5, 10, 15 and 20 minutes after Cu-64 infusions (30 µCi/µl, 667 nl total volume infused at 10 µl/hour) delivered into (**F**) an agarose phantom using a syringe pump, in rat brain through implanted S-MiNDS using (**G**) a syringe pump, and (**H**) an iPrecio pump. (**I**) Normalized ROI sum intensity table shown in (E).
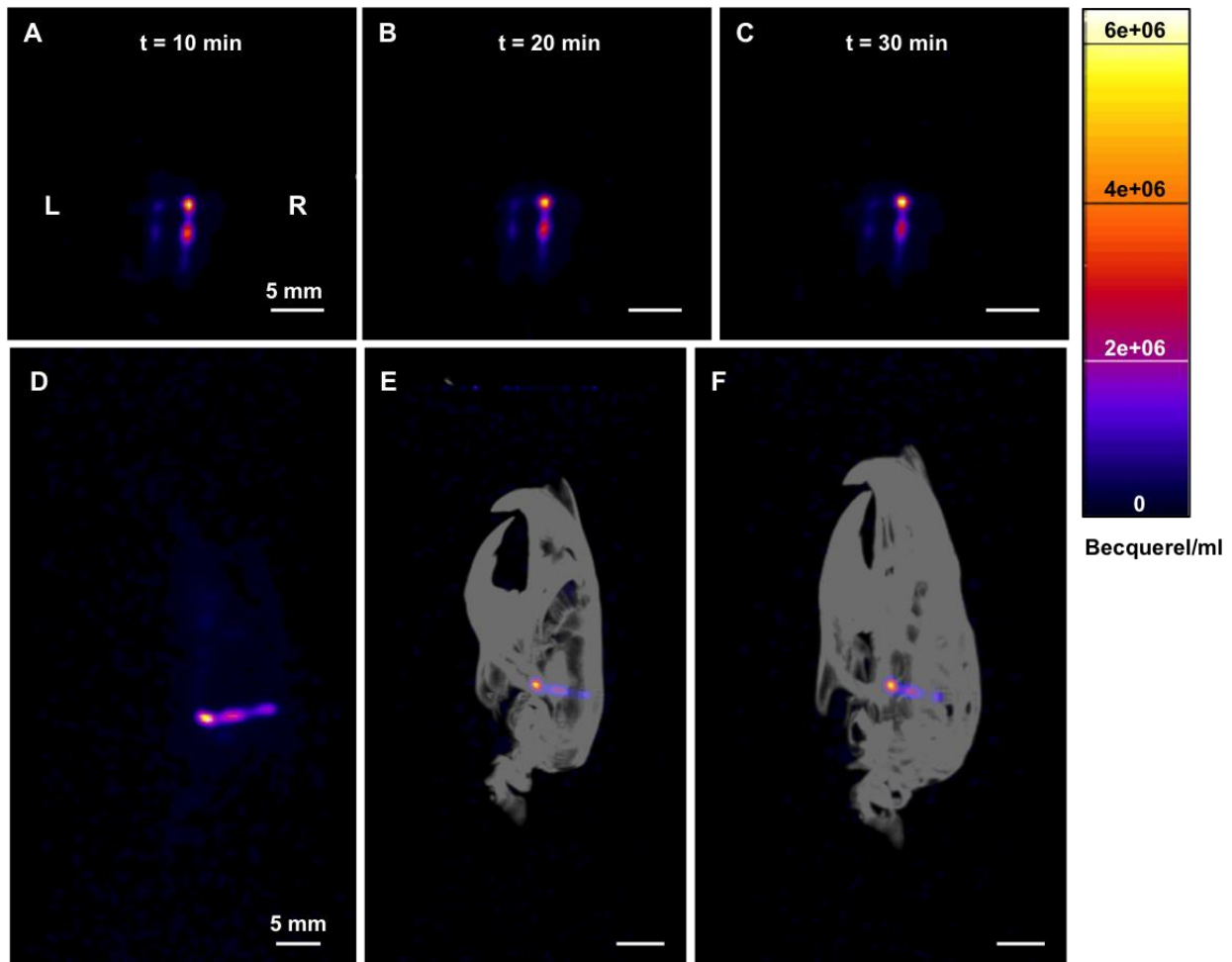
Fig. S14. Infusion intensity and projection characterization via PET. **(A, B, C)** Time sequence of PET images acquired at 10, 20, and 30 minutes after radioactive Cu-64 infusion, respectively. Radioactive Cu-64 (1 µCi/µl) was infused through using a 31G needle inserted stereotaxically into the right and left rat striatum. 2 µl were infused at 0.2 µl/minute on the right, and 200 nl were infused at 0.2 µl/minute on the left. **(D)** 3D reconstructed Maximum Intensity Projection (MIP) Image taken 35 minutes post-infusion. **(E, F)** 3D reconstructed Maximum Intensity Projection (MIP) image taken 35 minutes post-infusion with simultaneously imaged computed tomography (CT) overlaid.
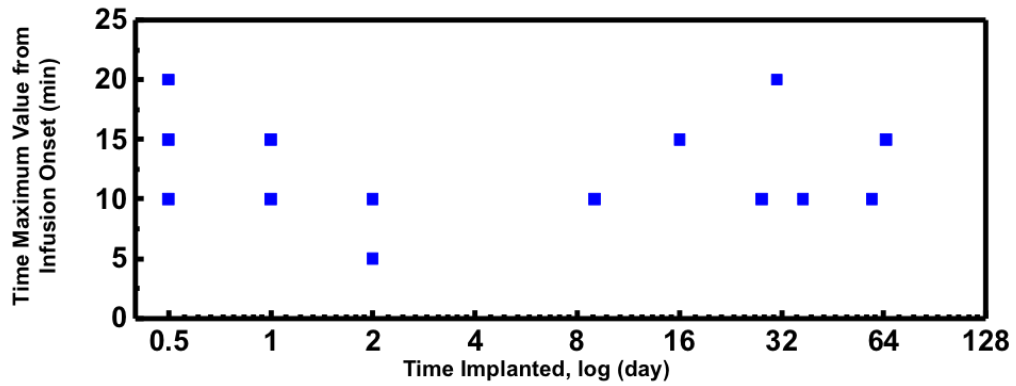
Fig. S15. PET imaging after pump implantation. Plot of length of time to reach maximum bolus value as measured using PET imaging vs time after implantation of MiNDS. Animals with implanted MiNDS underwent PET infusions at various post-implantation time points. Resistance to infusion due to implant failure or tissue gliosis was measured as the time to maximum value from infusion onset. A delay indicates resistance to infusion, due to possible occlusion of the microfluidic cannula. Time implanted was calculated from the date of surgery when MiNDS was implanted.
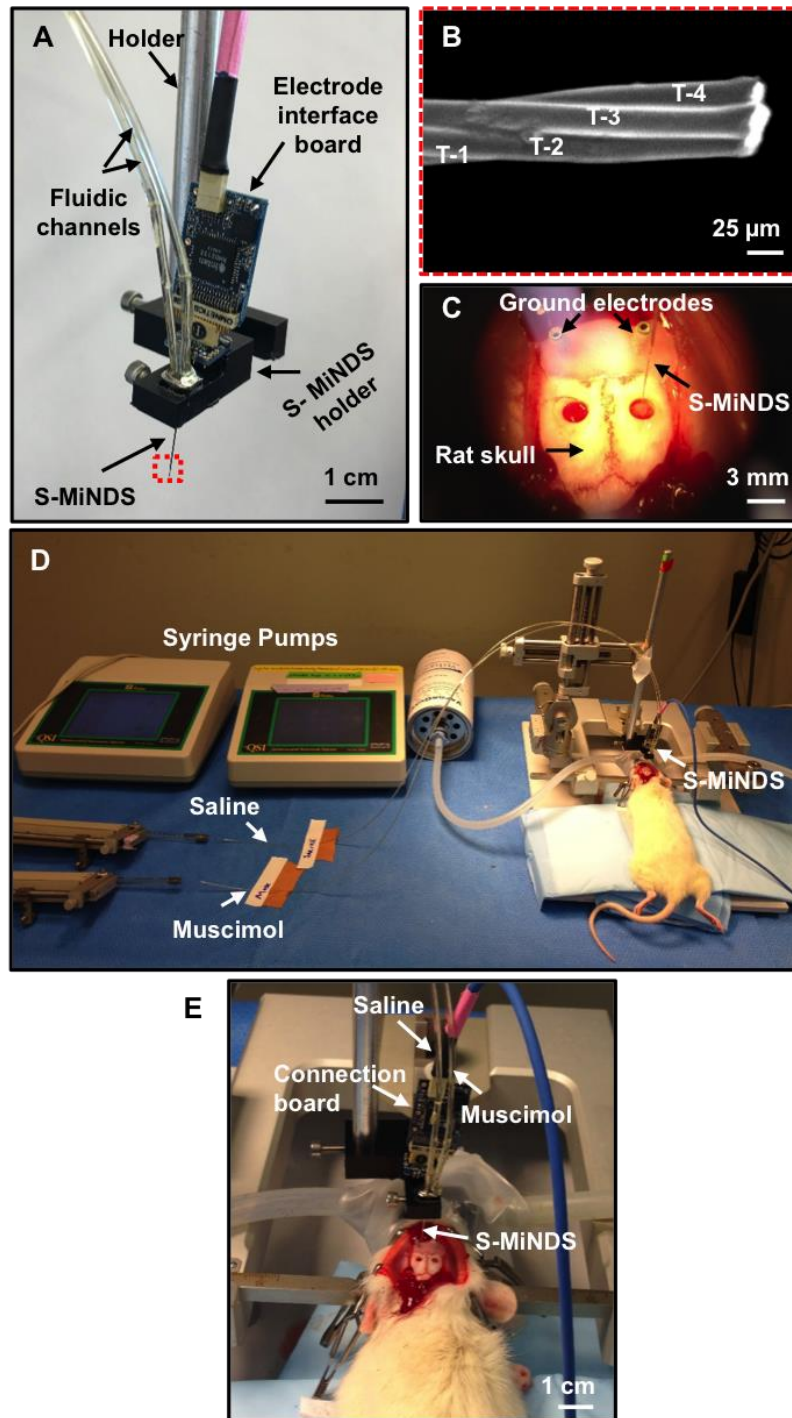
Fig. S16. Surgical procedure of an S-MiNDS with tungsten tetrode in vivo. (A) Image of experimental setup of the MiNDS with tetrode and electrode interface board. **(B)** SEM image of the tip of thetetrode (red dashed outline in (A)) consists of four individual tungsten electrodes (T-1, T-2, T-3, T-4). **(C)** A microscope image of the S-MiNDS inserted into the brain via a burr hole on the skull of a rat. (D, E) Images of **(D)** experimental setup and **(E)** MiNDS implantation into the head of a rat.
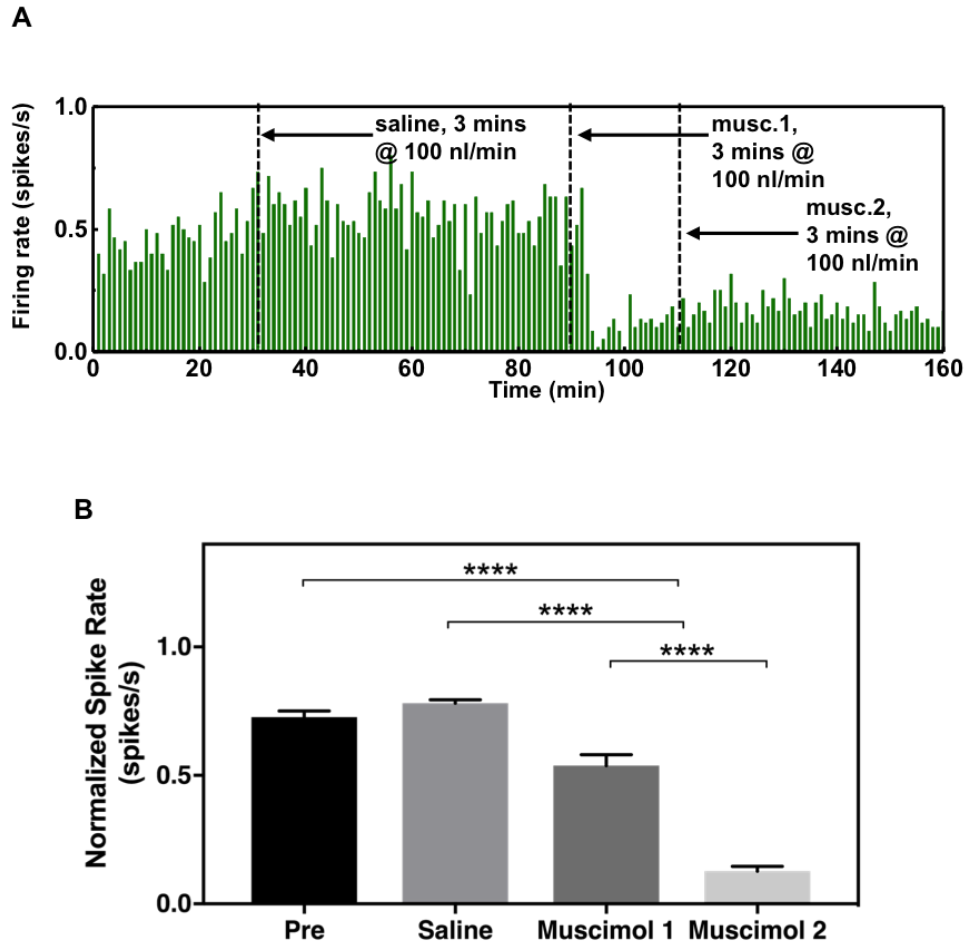
Fig. S17. Distinctive infusion effect on firing rate in a rat. (A) Unit rate histograms for 1 minute bins. The vertical black dashed lines indicate the start of saline infusion (at 30 minutes), the muscimol infusion (at 60 minutes), and the second muscimol infusion (at 90 minutes), respectively. **(B)** Averaged normalized spike rate for each infusion intervals for two rat trials shown in 3A and S17A. (n=2 rats; error bars represent standard error). Statistical analysis was done using one-way ANOVA followed by Tukey test ****$p<0.0001$.
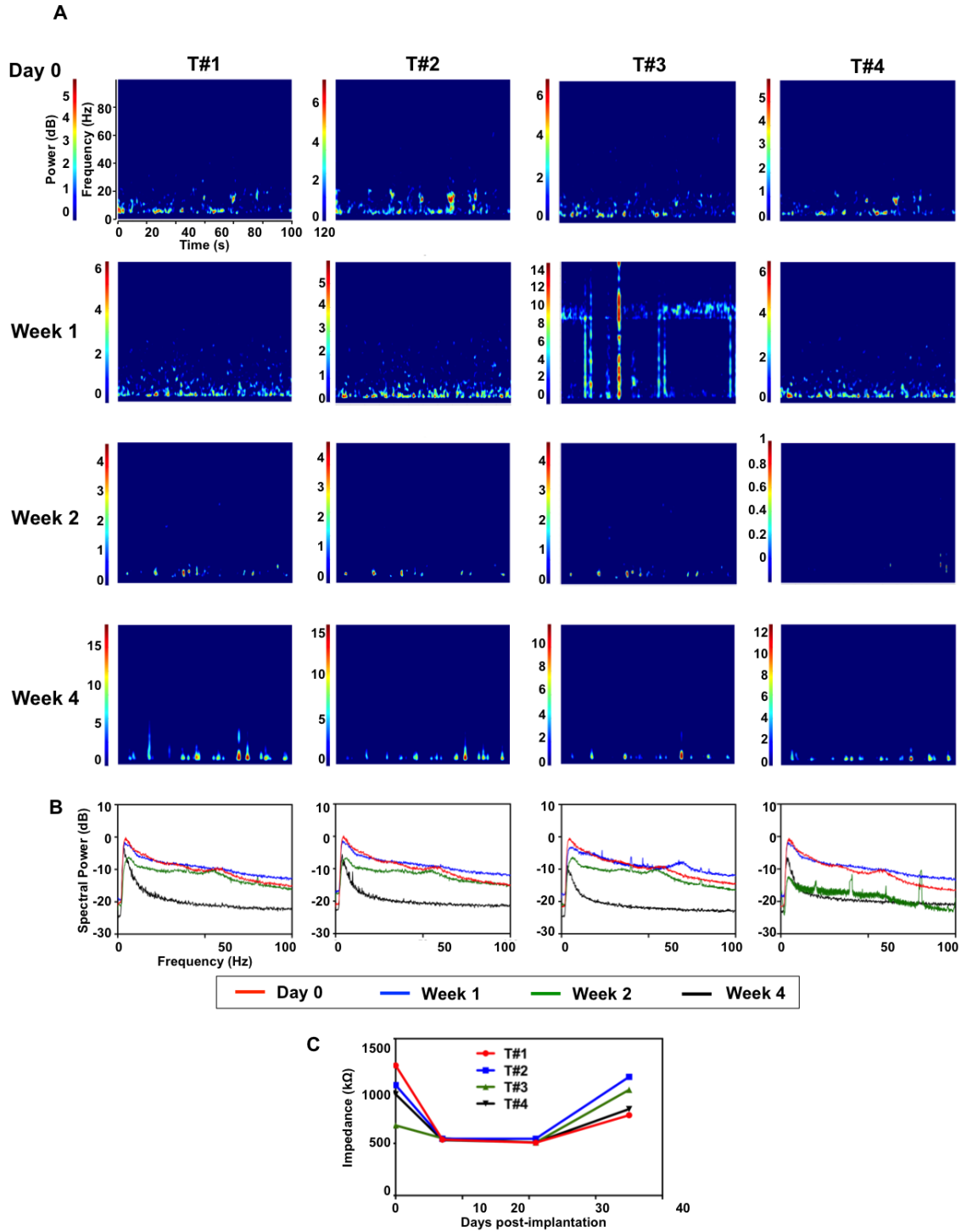
Fig. S18. Spectrograms from rat experiments. (**A**) Spectrograms obtained from each of four channels (T-1, T-2, T-3, T-4) from an implanted tungsten-tetrode in rat striatum at Day 0, Week 1, 2, and 4 after MiNDS implantation. (**B**) Power Spectral densities for each individual W electrode (T-1, T-2, T-3, T-4) at every time point. (**C**) Impedance values of each individual electrode at every time point.
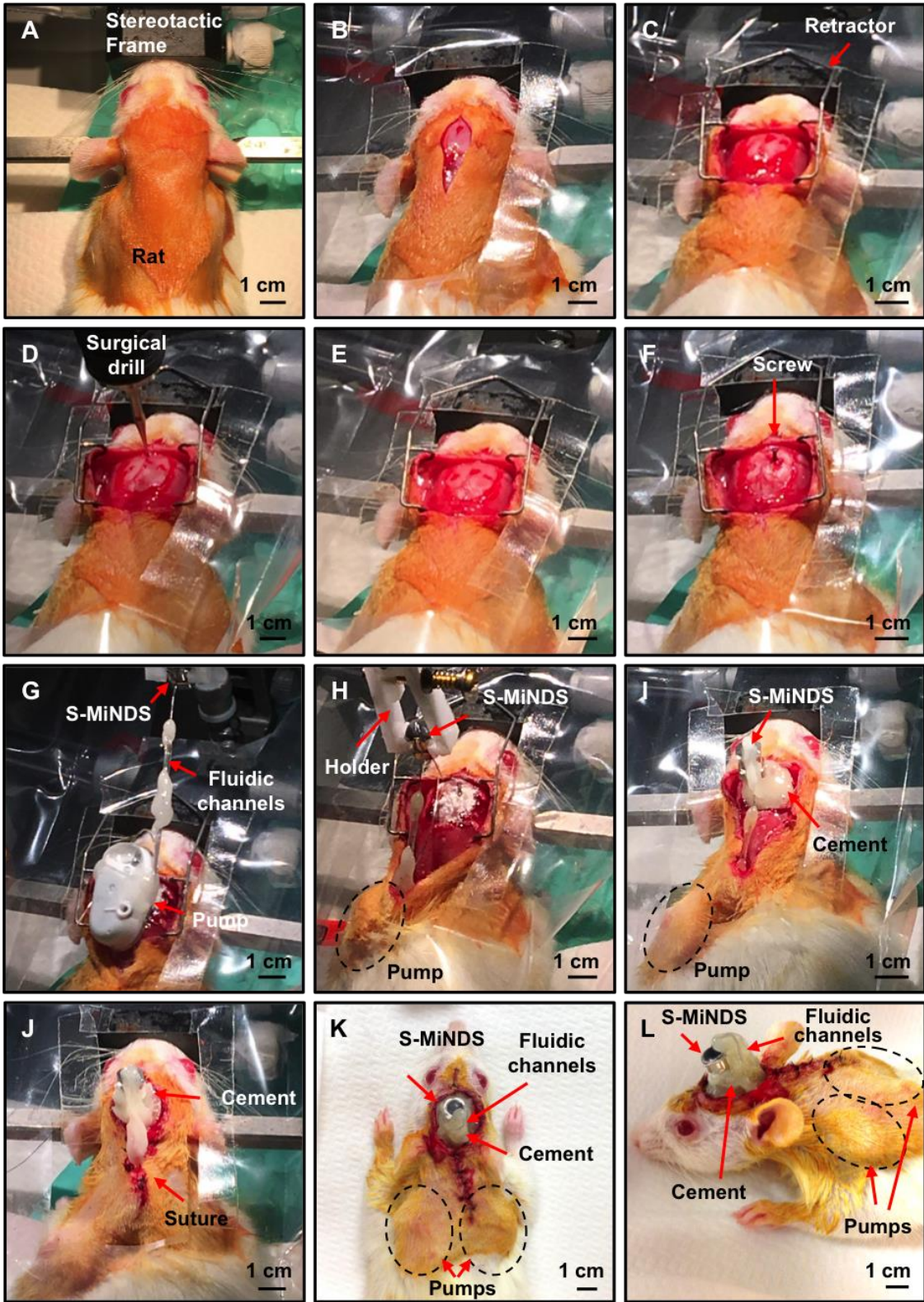
Fig. S19. Surgical procedure of an S-MiNDS and two pumps implantation in vivo. (A) The rat is mounted in a stereotactic frame and covered with sterile surgical drapes. (**B**) Initial incision is made with #15 scalpel blade, approximately 3 cm long. (**C**) Connective tissue is separated using cotton-tipped applicators, and the incision is maintained open using a surgical retractor. (**D, E**) A burr hole is made using a 0.7 mm drill bit, approximately 3 mm lateral and 4 mm posterior to the bregma. A 2nd larger burr hole is created using a 1 mm drill bit, 2.5 mm lateral and 5 mm posterior to the bregma. (**F**) A ground screw (0.043" diameter, 0.1" length, 100 TPI) is screwed into the smaller burr hole, such that the tip protrudes 0.2 mm into the dura, without piercing the brain. This screw acts as support for the cement and MiNDS. The C&B Metabond adhesive is applied using a brush applicator to the exposed skull surrounding the burr holes, to enable better cement bonding to the bone. (**G**) A subcutaneous pocket for the pump is created using blunt dissection, and the pump is inserted using the frame. (**H**) The MiNDS is slowly lowered 9 mm into the brain using a stereotactic frame. (**I**) Dental cement is used to cover the ground screw and plate, securing the MiNDS. The cement is allowed to dry, fixing the implants in place securely. (**J**) The skin surrounding the implant is closed using 5-0 monofilament non-resorbable suture and secured with 3M tissue glue. (**K**) Top view and (**L**) side view pictures of animal post-surgery.
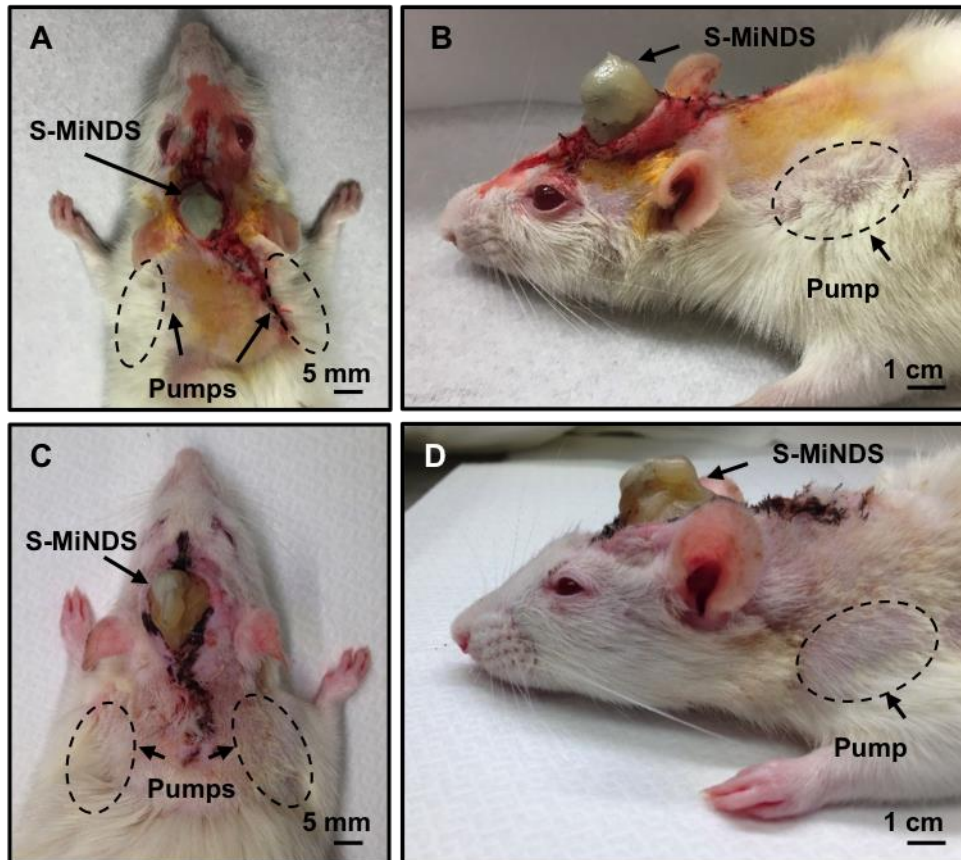
Fig. S20. Implanted pumps in a rat. (A-D) Top **(A, C)** and side images **(B, D)** of a rat implanted with two pumps and an S-MiNDS immediately post-surgery (A, B) and a week post-surgery (C, D).
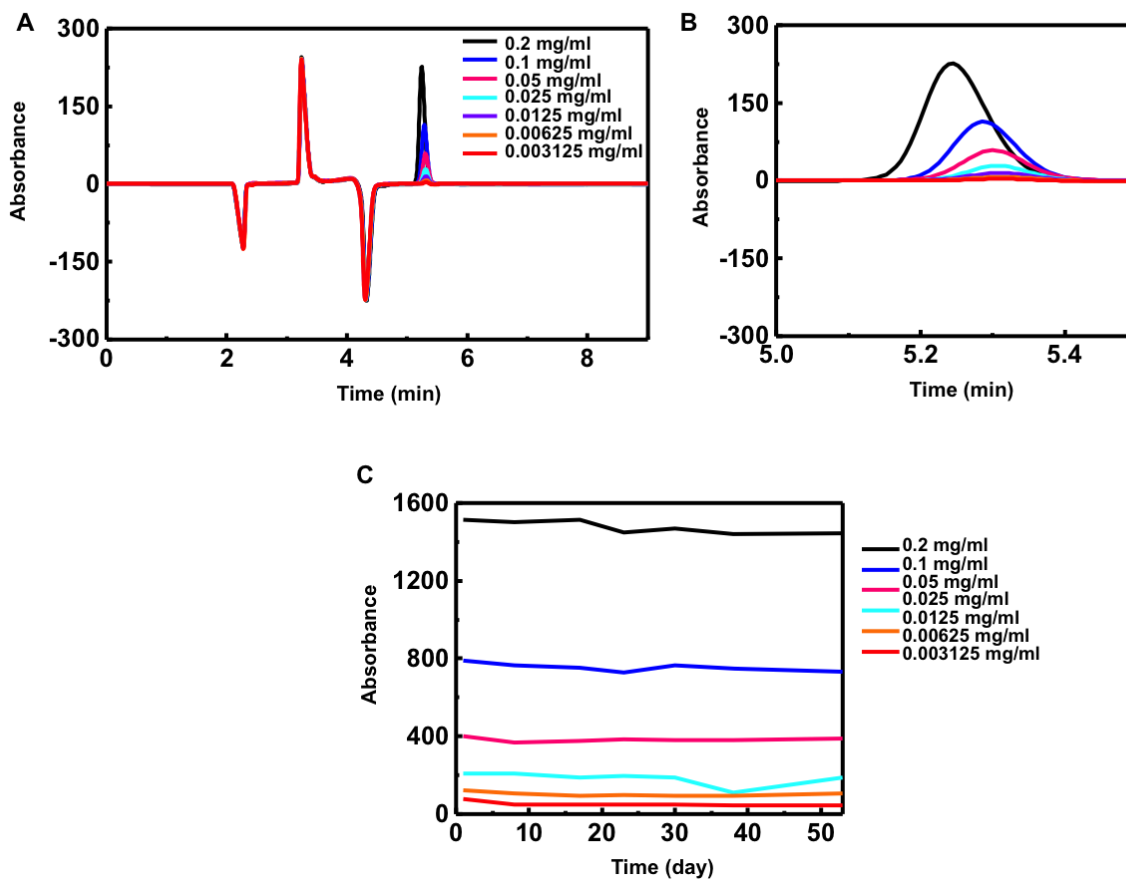
Fig. S21. High-performance liquid chromatography absorbance spectrum at various concentrations of muscimol. (**A**) HPLC absorbance spectrum eluted over time. The final peak decreases proportionally with muscimol concentration, and is used to assess muscimol stability over time. (**B**) Magnification of the final peak shown in (A). (**C**) HPLC absorbance of muscimol over time up to 54 days, at stock concentration of 0.2 mg/ml up to 6 serial dilutions (0.1, 0.05, 0.025, 0.0125, 0.00625, 0.003125 mg/ml).
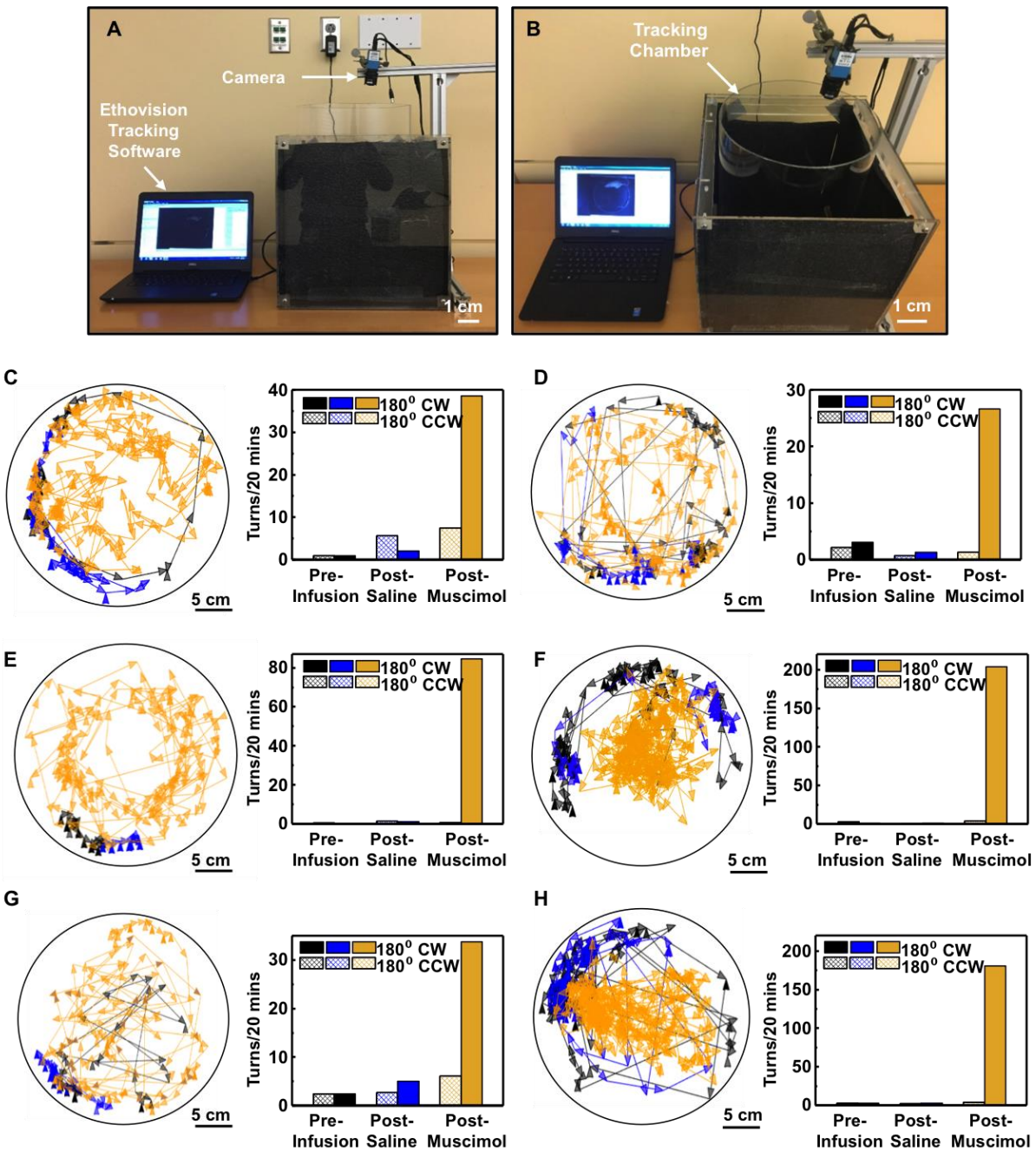
Fig. S22. Behavioral study on rat models. (A,B) A 1 ft diameter chamber was placed in an opaque cube, with dimensions 1.6'x1.6'x1.6'. An ethernet digital camera was placed above the chamber such that the entire chamber was within view. The camera was connected to a laptop containing the tracking software. Videos were first captured using IC capture software, and then analyzed using Ethovision behavioral testing software.**(C-H)** Color-tracking map of animals during the pre-infusion, post-saline, and post-muscimol infusions and corresponding average

number of 180° CW and CCW turns at pre-infusion, post-saline and post-muscimol infusion cases. Mean rotation rates in each interval is shown in Figure 3H. (n=3 rats, 2 trials/rat (Rat#1 trials: C, D; Rat#2 trials: E, F; Rat#3 trials: G, H. Error bars represent standard error). *$p<0.0332$, **$p<0.0021$). Statistical analysis was done using one-way ANOVA followed by Tukey test.
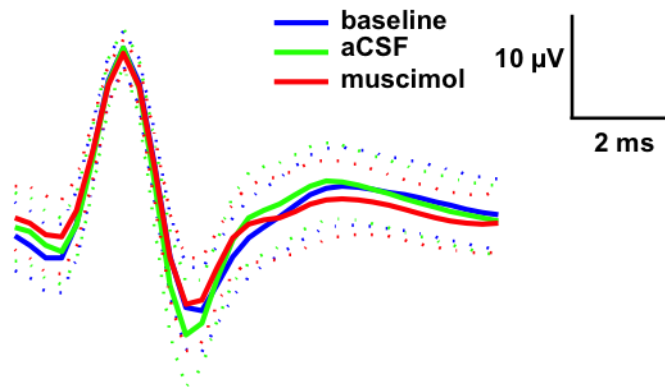
Fig. S23. Average waveforms during distinctive infusions in a NHP. Average waveforms for units binned during each period (pre-infusion baseline, aCSF infusion, and muscimol infusion) with standard deviation in dashed outlines.
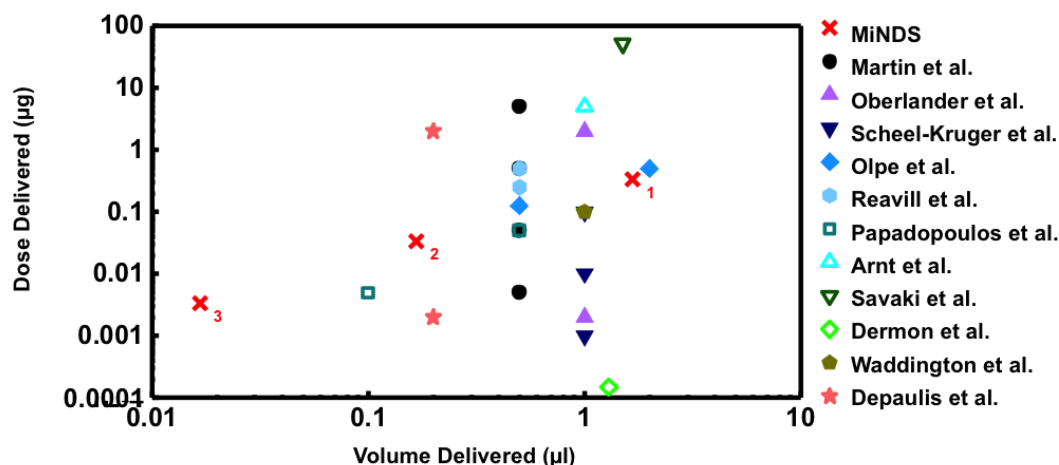
Treatment regions	Slope	SE	Slope - 2*SE	Slope+2*SE
Pre aCSF	0.736	0.005	0.725	0.746
Post aCSF	1.039	0.010	1.019	1.059
Post muscimol	0.250	0.001	0.248	0.253
Post aCSF2	3.854	0.066	3.723	3.986
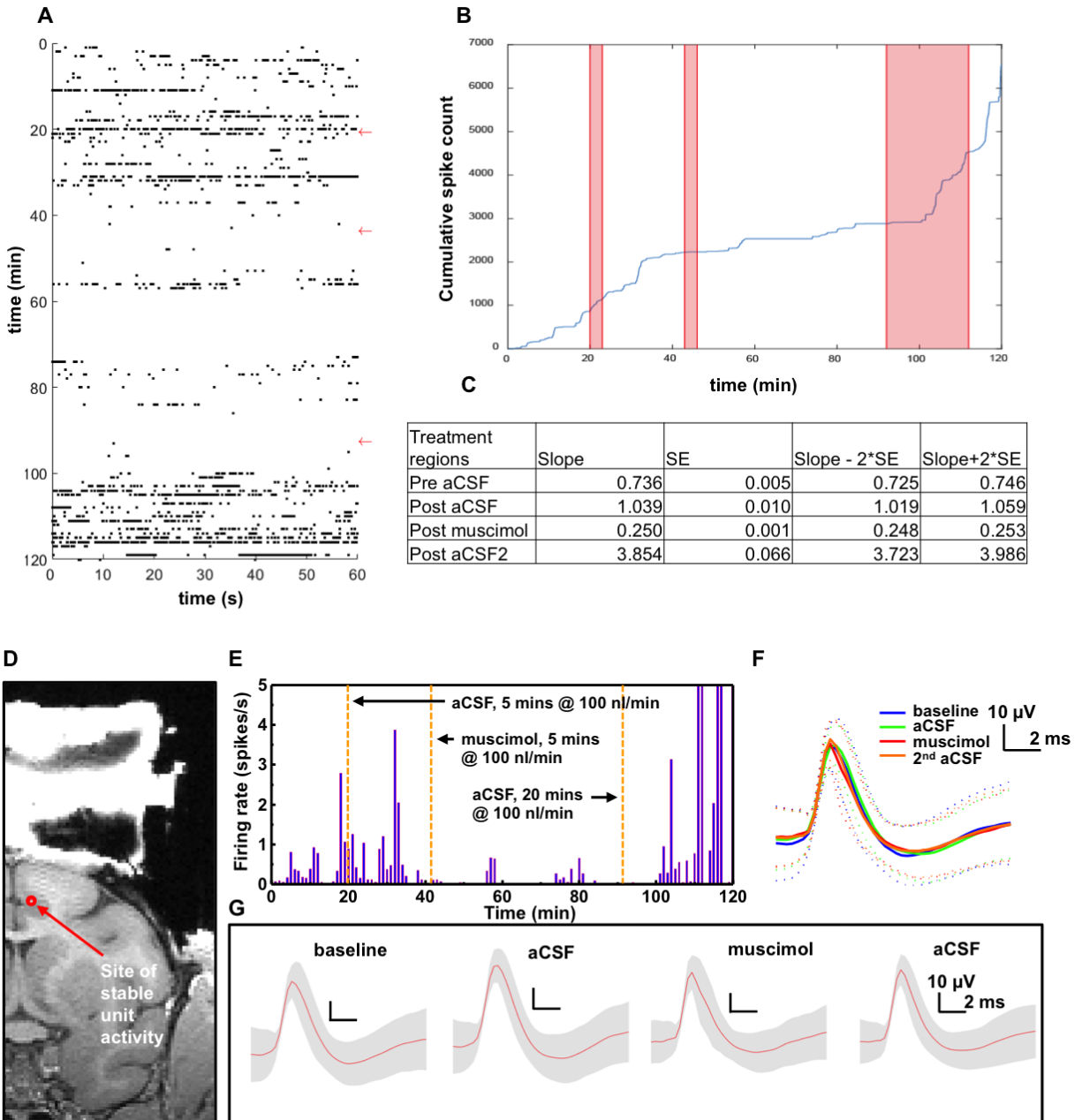
Fig. S24. Distinctive infusion effect on firing rate in a NHP. (A) Raster plot of spike activity for data plotted in (E). Red arrows mark beginning of infusion periods as marked in (E). **(B)** Cumulative sum of spike counts for data plotted in (E). Red vertical lines indicate infusion periods as marked in (E). **(C)** Table shows the values of slopes for linear fit lines for each treatment period and their standard error (SE) and confidence intervals. Red shaded regions are not included in analysis. **(D)** MRI image shows estimated location of the MiNDS infusion and recording. Estimated coordinates of the MiNDS tip are anterior posterior (AP) 21 mm and mediolateral (ML) 3 mm, which corresponds to the dorsal bank of the cingulate cortex. **(E)** Unit

firing rate histograms for 1 minute bins. Vertical orange dashed lines denote the start of aCSF or muscimol infusion. **(F)** Compiled average waveforms for units binned during each period (pre-infusion baseline, aCSF infusion, muscimol infusion, and 2nd aCSF infusion) with standard deviation in dashed outlines. **(G)** Average waveforms for units binned during each period (pre-infusion baseline, aCSF infusion, and muscimol infusion) with standard deviation in gray shading.
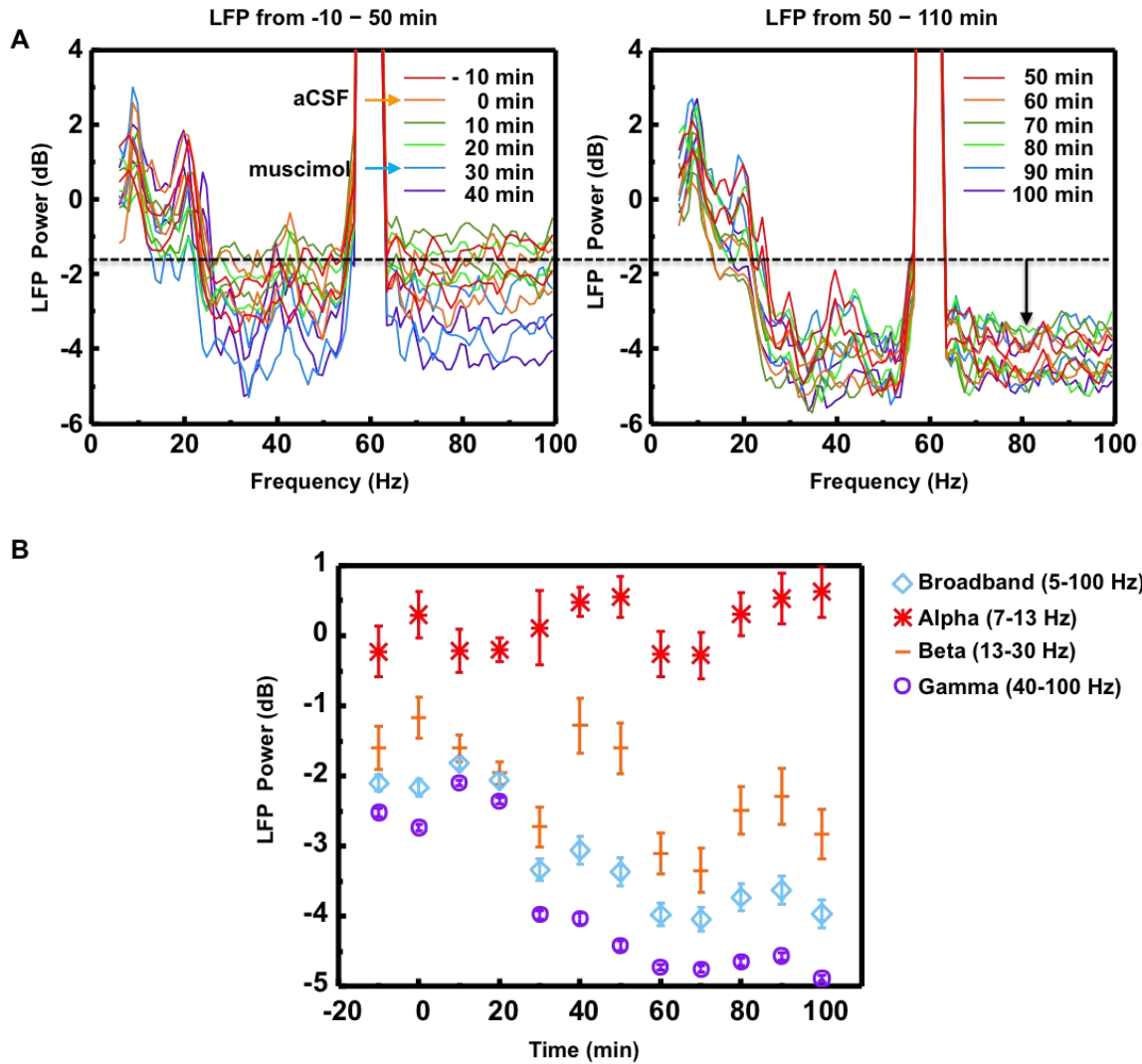
Fig. S25. LFP power analysis of a NHP trial. (**A**) Pink-fit LFP power (5 – 100 Hz) averaged over 10 minutes intervals through the course of first aCSF infusion (beginning at 0 minute), and muscimol infusion (beginning at 30 minutes) from signals recorded in Fig. 4. The pair of same colored curves represent 95% confidence interval margins of the measured LFPs. Colors of each pair of curves correspond to signals averaged over 10 minutes periods as labeled in the legend at the top right of each plot. (**B**) LFP power for different categorical spectral ranges (not including 53 – 65 Hz where line noise interferes with physiological signal) based on the plots showed in panel (A).

Fig. S26. Plot of dose/volume delivered in previous studies reported in the literature, injecting muscimol into the SN compared to MiNDS. All previous studies were conducted using acute needle insertion and injection on restrained or anesthetized animals. The MiNDS device reported here are obtained with chronically implanted system in a rat brain (x_1) using PET (x_2), and in vitro in water (x_3).

Experiment	Pre-aCSF-saline	Post-aCSF-saline	Post muscimol 1	Post muscimol 2	Post-saline 2
NHP #1					
average	1.97672	1.32009	0.0423		
standard deviation	2.26836	1.72872	0.20759		
p (chi value)		<.0001	<.0001		
NHP #2					
average	0.49649	0.57833	0.08188		
standard deviation	1.74045	2.00478	0.63517		
p (chi value)		<.01	<.0001		
Rat #1					
average	12.75303	11.56864	10.58218	0.00000	0.00000
standard deviation	3.13337	3.02211	2.70410	0.00000	0.00000
p (chi value)		<.0001	<.0001	<.0001	1.00000
Rat #2					
average	0.43254	0.57000	0.55367	0.14598	0.15312
standard deviation	0.88884	1.12797	1.03158	0.40891	0.41491
p (chi value)		<.0001	1.00000	<.0001	1.00000

Table S1. Statistical analysis for muscimol inhibition of spike activity for two sessions in two rats and for two sessions in a NHP. Tabulated metrics were performed by summing spikes for baseline (pre-infusion), post-aCSF (monkey) or saline (rat) infusion, and post-muscimol infusion periods and dividing by these periods (variable for each session). Mean spike rates (spikes/second), standard deviations, and chi squared values were calculated with these values.